PROJECT ACRONYM: **FutureAgriculture**

PROJECT TITLE: **Transforming the future of agriculture through synthetic photorespiration**

Deliverable 1.5

Model of plant photosynthesis

TOPIC			**H2020-FETOPEN-2014-2015-RIA**
GA			**686330**
CONTACT PERSON			**Arren Bar-Even** Bar-Even@mpimp-golm.mpg.de
NATURE	Report (R)	**DISSEMINATION LEVEL**	PU
DUE DATE	31/12/2018	**ACTUAL DELIVERED DATE**	14/12/2018
AUTHOR			Christian Edlich-Muth

This project has received funding from the European Union's Horizon 2020 research and innovation programme under grant agreement No 686330.

Table of Revisions

REVISION NUMBER	DATE	WORK PERFORMED	CONTRIBUTOR(S)
1	05/12/2018	Document preparation	MPIMP
2	06/12/2018	Formatting	IN
3	13/12/2018	Revision	Consortium

Contents

1 Executive Summary **5**

2 Cooperation between participants **6**

3 Core report **7**

3.1 Theory 7

3.1.1 Pathways 7

3.1.2 The stoichiometric consumer model of photosynthesis 9

3.1.3 Stoichiometric-kinetic model 13

3.1.4 Physicochemical parameters 24

3.2 Results 27

3.2.1 Parameters and variables 27

3.2.2 Rubisco kinetics 28

3.2.3 Limitation by light 30

3.2.4 Limitation by enzyme activities other than Rubisco 31

3.2.5 Limitation by a Calvin cycle enzyme 31

3.2.6 Limitation by a photorespiratory enzyme 34

3.2.7 Limitation by a photorespiration carboxylase 35

4 Conclusions **37**

Table of Charts

1 Bypass coefficients 11

2 Flux distribtion of the Calvin cycle and photorespiratory bypasses 20

3 Kinetic constants of Rubisco and carbon dioxide diffusion 28

4 Calvin cycle enzyme total activities 33

Table of Figures

1 Energy requirements of native photorespiration and the Calvin cycle 7

2 Energy requirements of synthetic photorespiration shunts 8

3 The consumer model of photosynthesis 10

4 Rubisco kinetics and net carbon fixation rates in the consumer model 29

5 Light response curves of the restricted kinetic-stoichiometric model 31

6 Limitation by a Calvin cycle enzyme 32

7 Limitation by a photorespiration enzyme 34

8 Limitation by a photorespiration carboxylase 36

1 Executive Summary

A model of C3 plant photosynthesis was developed that predicts the effects of replacing native photorespiration with synthetic shunts on the net carbon fixation rate. The model adopts the approach of Farruqar, von Caemmerer and Berry [1] which combines a phenomenological treatment of the light reactions with a largely stoichiometric treatment of the Calvin cycle with the exception of Rubisco and CO2 diffusion. We have generalized this model so that it can apply to all of our - and potentially many other - synthetic photorespiration shunts.

The model directly or indirectly incorporates the most important environmental variables, such as light and water availability. The predictions of the model are unequivocal in that replacing native photorespiration with a carbon-neutral or carbon-positive shunt will increase net carbon fixation considerably in all environmental conditions. The benefits are expected to highest, relative to native photorespiration, when the conditions are the most difficult, i.e. in drought.

In addition to demonstrating the benefits of photorespiration shunts when light or the activity of Rubisco are limiting, we investigated what activities of Calvin cycle enzymes and photorespiration shunt enzymes would be necessary in order to not be limiting. We demonstrate that many of our synthetic shunts would disburden all critical Calvin cycle enzymes, and thereby increasing net carbon fixation in situations where these enzymes would otherwise be limiting.

In this report, we include a full mathematical derivation of the model and the applications of all the above to native photorespiration, the published glycerate shunt and five of our synthetic shunts (arabinose 5-phosphate shunt, ribulose 1-phosphate shunt, erythrulose shunt, xylulose shunt and tartronyl-CoA shunt).

2 Cooperation between participants

All of the work resulting in this deliverable was performed by MPIMP. However, all partners participated in discussions that helped improve the deliverable.

3 Core report

3.1 Theory

Our aim is to develop a framework for modeling C3 photosynthesis (PS) in mesophyll cells that allows us to compare native photorespiration (PR) with engineered photosynthetic shunts. In particular, we want to model conditions that are most relevant to agricultural crops, i.e. a range of light intensities and both ambient and low CO_2 intercellular airspace concentrations. The latter can for example occur in drought when the plant closes its stomata.

3.1.1 Pathways

The pathways we are concerned with are the Calvin cycle, native photorespiration, the published tartronic glycerate pathway [2] and the synthetic ribulose 1-phosphate (Ru1P), arabinose 5-phosphate (Ar5P), erythrulose (Eu), xylulose (Xu) and tartronyl CoA (TrCoA) shunts.

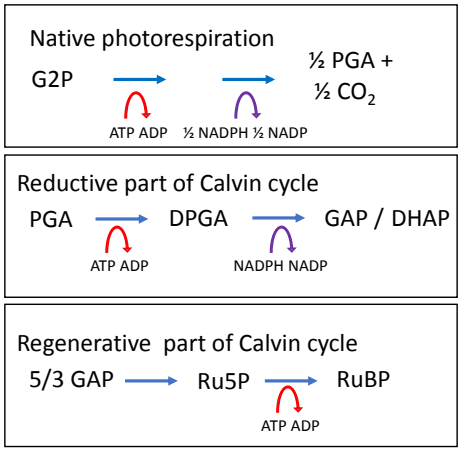

Figure 1: Energy requirements of native photorespiration and the Calvin cycle. Summary of energy consumption of native photorespiration, the reductive and regenerative Calvin cycle.

The analysis of energy requirements of photorespiration shunts is not straight-forward. Simply counting the number of ATPs and NADPHs that are consumed in a pathway can be misleading. For example, native photorespiration converts one molecule of G2P into half a molecule of PGA, consuming 1 ATP and 0.5 NADPHs in the process (0.5 ATP for re-fixing 0.5 units of ammonia, 0.5 ATP for phosphorylating 0.5 units of glycerate and 0.5 NADPH for reducing 0.5 units of hydroxypyruvate; 0.5 NADH are generated in the glycine cleavage complex but cancel with the 0.5 units of NADH that are required to regenerate the donor of the transaminase reaction, e.g. glutamate from 2-oxoglutarate). The difficulty arises if we try to compare this number to e.g. a carbon-neutral pathway like the Ru1P pathway. We can count the number of ATPs and NADPHs easily enough but it does not make any sense to compare them to native photorespiration because the product of the Ru1P pathway is RuBP, not PGA.

The solution is to calculate the number of ATPs and NADPHs that are required to regenerate one molecule of RuBP from the products of RuBP oxygenase, PGA and G2P. However, this raises the

issue of how to deal with the fact that e.g. native photorespiration is 'carbon negative' - 0.5 units of CO_2 (i.e. 1/6 of a molecule of GAP) are lost, so we cannot regenerate a full molecule of RuBP. We deal with this by making the reasonable assumption that the missing amount of GAP is supplied by the Calvin cycle.

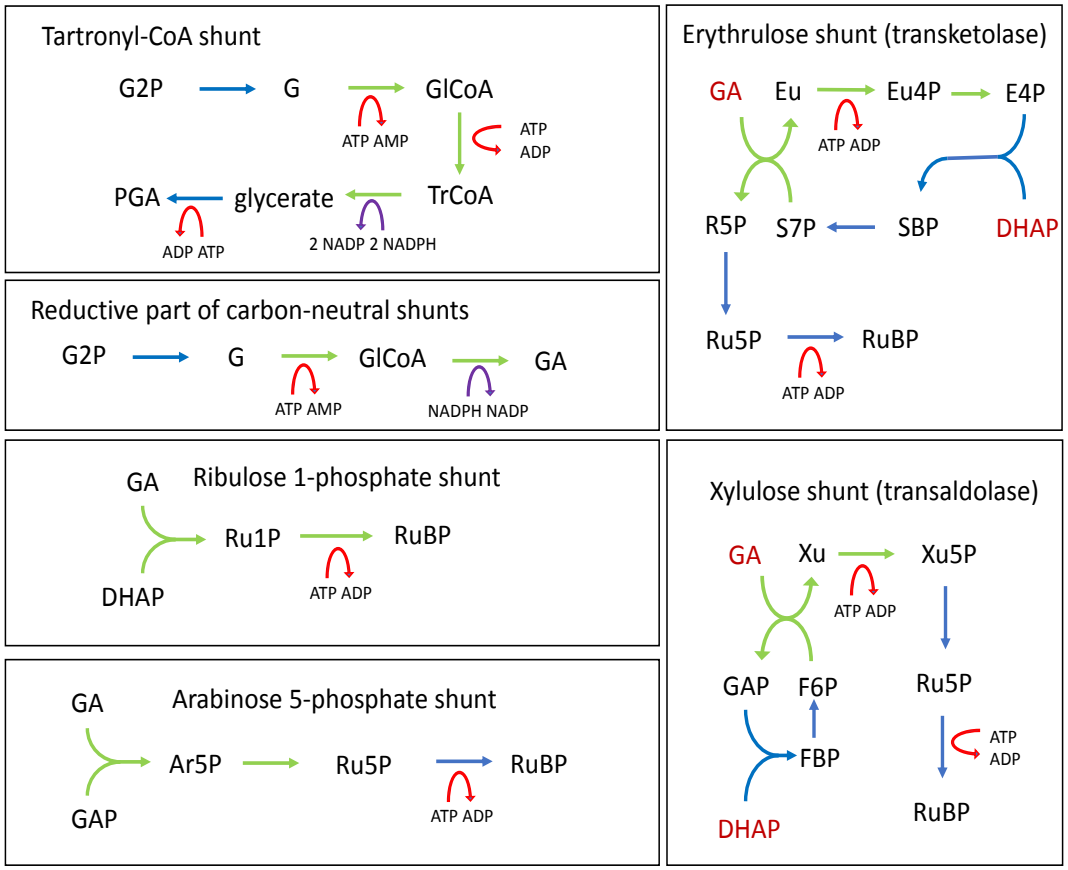

Figure 2: Energy requirements of synthetic photorespiration shunts. The carbon-positive tartronyl-CoA shunt converts G2P to PGA. The regenerative phase (from PGA to RuBP) is identical to the Calvin cycle. The four carbon-neutral shunts consist of a generic reductive phase, followed by individual regenerative phases. In the reductive phase, glycolaldehyde (GA) is made from glycolate 2-phosphate (G2P) and in the regenerative phase, GA is combined with either GAP or DHAP to regenerate RuBP. Green arrows indicate non-native reactions, and blue arrows native Calvin cycle or photorespiration reactions.

This description is extremely useful as it allows the comparison of any photorespiration shunt both with one another and native photorespiration. The energy requirements of native photorespiration are calculated in the following manner. G2P is converted to 0.5 PGA consuming 1 ATP and 0.5 NADPH in the process. Together with the molecule of PGA that is also produced by RuBP oxygenase, we have 1.5 PGA which require 1.5 ATP and 1.5 NADPH to form 1.5 molecules of GAP. Now the Calvin cycle supplies the missing 1/6 of a molecule of GAP so that 5/3 GAP + 1 ATP can be converted back to RuBP. All in all 3.5 ATPs and 2 NADPHs have been consumed to achieve this.

The same analysis for the tartronyl-CoA pathway is as follows: G2P is converted to PGA consuming 4 ATPs (2 by CoA synthetase, 1 by the carboxylase and 1 by glycerate kinase) and 2 NADPHs. Together with the molecule of PGA that is also produced by RuBP oxygenase, we have 2 PGA which require 2 ATP and 2 NADPH to form 2 molecules of GAP. The excess 1/3 of a GAP (equivalent to one fixed

and reduced CO_2) is exported from the chloroplast so that 5/3 GAP + 1 ATP can be converted back to RuBP. All in all 7 ATPs and 4 NADPHs have been consumed to achieve this.

For the Ru1P, Ar5P, Erythrulose and Xylulose shunts the narrative is different: in the reductive part that all carbon-neutral shunts share, G2P is converted to GA consuming 2 ATPs and 1 NADPH. The molecule of PGA that is also produced by RuBP oxygenase, consumes 1 ATP and 1 NADPH to form 1 molecules of GAP or DHAP in the reductive part of the Calvin cycle. The two molecules are then combined, to form a pentose phosphate that is ultimately converted to RuBP. In the Ru1P shunt, DHAP and GAP form Ru1P in an aldolase reaction; Ru1P is phosphorylated to RuBP. All in all we have consumed 4 ATPs and 2 NADPHs. The Ar5P shunt is a variation on this theme, also consuming 4 ATPs and 2 NADPHs. In contrast, the Erythrulose shunt forms erythrulose in a transketolase reaction. Erythrulose is phosphorylated and isomerised to E4P. E4P is then condensed with DHAP to form SBP which is dephosphorylated to S7P, the donor of the transketolase reaction. Ultimately, what remains is one molecule of ribose 5-phosphate (R5P) which is converted to Ru5P and finally RuBP. Since an additional phosphorylation (erythrulose kinase) / dephosphorylation (SBPase) occurs, one more unit of ATP is consumed than in the Ru1P/Ar5P shunts. The Xylulose shunt also requires the additional expense of one ATP compared to Ru1P/Ar5P because the regeneration of F6P as the substrate of the transaldolase reaction proceeds via FBP.

3.1.2 The stoichiometric consumer model of photosynthesis

Thus, native photorespiration, each of the synthetic photorespiration shunts, and the Calvin Cyle proper, can be understood as isolated cycles that regenerate RuBP and either fix or release CO_2 in the process and thereby produce or consume triose phosphates at the same time (Fig. 3). From this viewpoint, native photorespiration is the process that converts RuBP and one sixth of a molecule of GAP back into one molecule of RuBP plus 0.5 molecules of CO_2, consuming 3.5 ATPs and 2 NADPHs in the process. The intermediates, e.g. PGA and glycolate-2-phosphate, are irrelevant in this description because they are made and consumed in equal amounts. Moreover, by balancing CO_2 with GAP in each of the pathways, we obtain catalytic cycles for photosynthesis, native photorespiration and synthetic photorespiration shunts that do not depend on one another to supply intermediates.

The most important consequence of this description is that despite the fact that native/synthetic photorespiration on the one hand and photosynthesis on the other share some enzymes and metabolic intermediates, the two processes can now be separated and treated in isolation.

Each catalytic pathway that regenerates RuBP is characterised by just three numbers: the number of CO_2 molecules that are consumed (α, can be negative) per turn of the cycle, the number of ATP molecules that are consumed (β) per turn of the cycle and the number of NADPH molecules that are consumed (γ) per turn of the cycle (Table 1). These numbers have to be obtained from the detailed description of the actual pathways(Fig. 1 and 2).

We call this model the consumer model of photosynthesis, since it omits a description of the supply of CO_2 (via diffusion), ATP and NADPH (from the light reactions). The consumer model assumes that supply rates of CO_2, ATP and NADPH are infinite and therefore not limiting. A supply-demand steady-state model is presented in Section 3.1.3.

When only the consumption (but not the supply) of CO_2 is taken into account, the net carbon fixation rate is defined as the sum of the activities of Rubisco carboxylase ($v^{\dagger}_{carb}$) and oxygenase ($v^{\dagger}_{ox}$), weighted by the parameters α_0 and α respectively.

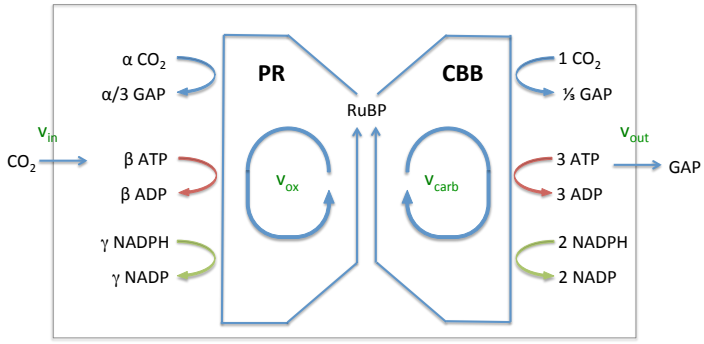

Figure 3: The consumer model of photosynthesis. The Calvin cycle (CBB, right) and photorespiration (PR, left) are conceptualised as catalytic loops that regenerate RuBP independently of each other. Three stoichiometric coefficients, (α, β and γ) fully define the properties of a pathway. α (can be negative) is the number of CO_2 molecules, β is the number of ATP molecules and γ is the number of NADPH molecules that are consumed per turn of the cycle (see Table 1). The total amount of CO_2, ATP or NADPH consumed can be calculated by multiplying the appropriate stoichiometric coefficient with the flux through RuBP oxygenase in photorespiration (v_{ox}) or RuBP carboxylase in the Calvin Cyle (v_{carb}). The sum of these two processes describes the total amount of CO_2, ATP or NADPH consumed. For example, total ATP consumption is $3\,v_{carb} + \beta\,v_{ox} = 3\,v_{carb} + 3.5\,v_{ox}$ in native photorespiration.

$$A^\dagger = \alpha_0\, v^\dagger_{carb} + \alpha\, v^\dagger_{ox} = v^\dagger_{carb} + \alpha\, v^\dagger_{ox} \tag{1}$$

The number of carbons that are consumed per turn of the Calvin Cyle is $\alpha_0 = 1$, while per turn of the native photorespiration cycle, 0.5 units of CO_2 are released, which is accounted for in our notation as $\alpha = -0.5$. In contrast a carbon-neutral shunt, as the name suggest, has $\alpha = 0$, and a carbon-fixing shunt has $\alpha = 1$. We use the † superscript here and in the following to signify that Eq. 1 refers to the consumer model only. The corresponding rate A without superscript is described in the full model that also takes into account limitations imposed by the supply of CO_2, ATP and NADPH.

The overall number of ATP or NADPH molecules that are consumed is calculated in a similar way, simply by replacing α_0 and α with β_0 and β or γ_0 and γ in Eq 1, respectively.

$$N^\dagger_{atp} = \beta_0\, v^\dagger_{carb} + \beta\, v^\dagger_{ox} = 3\, v^\dagger_{carb} + \beta\, v^\dagger_{ox} \tag{2}$$

$$N^\dagger_{nadp} = \gamma_0\, v^\dagger_{carb} + \gamma\, v^\dagger_{ox} = 2\, v^\dagger_{carb} + \gamma\, v^\dagger_{ox} \tag{3}$$

The two numbers $N^\dagger_{atp}$ and $N^\dagger_{nadp}$ therefore describe the number of ATP and NADPH molecules that are consumed by the Calvin Cyle and a given photorespiration pathway, be it native or a synthetic shunt. These two numbers, like $A^\dagger$, depend on the rates $v^\dagger_{carb}$ and $v^\dagger_{ox}$ that depend in turn on the kinetic parameters of Rubisco and the concentrations of CO_2 and O_2 in the chloroplast.

Pathway	α	β	γ
Native photorespiration	-0.5	3.5	2
Tartronic semialdehyde shunt	-0.5	3	1
Ribulose 1-P shunt	0	4	2
Arabinose 5-P shunt	0	4	2
Erythrulose shunt	0	5	2
Xylulose shunt	0	5	2
Tartronyl-CoA shunt	1	7	4
Calvin cycle	1	3	2

Table 1: Bypass coefficients. The coefficient α describes how many units of CO_2 are fixed per cycle, β and γ describe how many ATPs and NADPHs respectively are consumed in each cycle. The values of the Calvin cycle, denoted with the subscript '0', are $\alpha_0 = 1$, $\beta_0 = 3$ and $\gamma_0 = 2$.

Energy balance at a fixed oxygenation to carboxylation ratio

We describe three performance measures that allow the comparison of a synthetic shunt with native photorespiration when one or the other operates alongside the Calvin Cyle.

The first performance measure defines the number of units of CO_2 that are fixed on average per reaction of Rubisco. The other two describe the number of units of CO_2 that are fixed on average per molecule of ATP or NADPH consumed. These averages can be quickly derived if one assumes a fixed oxygenation proportion, $\rho = v^\dagger_{ox}/(v^\dagger_{carb} + v^\dagger_{ox})$, for example $\rho = 0.25$. This is a representative value at ambient CO_2 partial pressure, open stomata and saturating light. The value of $\rho = 0.25$ can be interpreted as meaning that, on average, every fourth reaction of Rubisco is oxygenating, while the three remaining ones are carboxylating (the ratio $v^\dagger_{ox}/v^\dagger_{carb} = 0.33$). First we calculate the number of CO_2 molecules that are fixed on average per Rubisco reaction. By 'average' we mean the expected number of fixed CO_2 molecules per reaction of Rubisco given that the probability of oxygenation is equal to ρ and the probability of carboxylation is equal to $1 - \rho$. To this end we divide $A^\dagger$ (Eq. 1) by the total activity of Rubisco, $v^\dagger_{carb} + v^\dagger_{ox}$, and use the definition of ρ:

$$\varepsilon^\dagger_{CO_2} = \frac{A^\dagger}{v^\dagger_{carb} + v^\dagger_{ox}} = \alpha_0 \cdot \frac{v^\dagger_{carb}}{v^\dagger_{carb} + v^\dagger_{ox}} + \alpha \cdot \frac{v^\dagger_{ox}}{v^\dagger_{carb} + v^\dagger_{ox}} = \alpha_0 \, (1 - \rho) + \alpha \, \rho \tag{4}$$

We call the performance measure $\varepsilon^\dagger_{CO_2}$ the carbon efficiency of the consumer model. It is positively correlated with α. For $\rho = 0.25$, $\varepsilon^\dagger_{CO_2}$ is 0.63 for native photorespiration and the glycerate shunt, 0.75 for the carbon-neutral and 1.0 for the carbon-fixing shunts. The carbon-neutral and carbon-fixing shunts are therefore at least 20 and 60% better, respectively, than native photorespiration with respect to carbon efficiency of the consumer model, i.e. given a fixed ratio ρ of oxygenation and no limitation by the supply of CO_2, ATP of NADPH.

Next we calculate the average number of ATPs per reaction of Rubisco that are consumed in photorespiration and the Calvin Cyle to regenerate RuBP. This is achieved by dividing $N^\dagger_{atp}$ (Eq. 2) by the total activity of Rubisco, $v^\dagger_{carb} + v^\dagger_{ox}$:

$$\nu^{\dagger}_{atp} = \frac{\beta_0\, v^{\dagger}_{carb} + \beta\, v^{\dagger}_{ox}}{v^{\dagger}_{carb} + v^{\dagger}_{ox}} = \beta_0\,(1-\rho) + \beta\,\rho \tag{5}$$

This average in itself it not very useful because it is only meaningful in relation to how many units of CO_2 are fixed on average per reaction of Rubisco. Therefore, to arrive at ATP efficiency, i.e. the number of CO_2 fixed per ATP, we need to divide the carbon efficiency $\varepsilon^{\dagger}_{CO_2}$ by $\nu^{\dagger}_{atp}$:

$$\varepsilon^{\dagger}_{atp} = \frac{\varepsilon^{\dagger}_{CO_2}}{\nu^{\dagger}_{atp}} = \frac{\alpha_0\,(1-\rho) + \alpha\,\rho}{\beta_0\,(1-\rho) + \beta\,\rho} \tag{6}$$

ATP efficiency is a function of α, β and ρ. For $\rho = 0.25$, the ATP efficiencies of native photorespiration and glycerate shunt are 0.2 and 0.21 (i.e. 5.0 and 4.8 ATPs are needed to fix one CO_2) respectively. All synthetic shunts are more ATP efficient, the Ru1P/Ar5P shunts by 15% ($\varepsilon^{\dagger}_{atp} = 0.23$, 4.33 ATPs per CO_2 fixed) and the tartronyl-CoA shunt by 25% ($\varepsilon^{\dagger}_{atp} = 0.25$, 4.0 ATPs per CO_2 fixed). The Erythrulose and Xylulose shunts are as ATP efficient as the glycerate shunt. This shows that a higher ATP cost in the photorespiration shunts (i.e. $\beta \cdot \rho$) is more than compensated by the higher carbon efficiency.

If we follow the same procedure for NADPH instead of ATP, we arrive at

$$\nu^{\dagger}_{nadp} = \frac{\gamma_0\, v^{\dagger}_{carb} + \gamma\, v^{\dagger}_{ox}}{v^{\dagger}_{carb} + v^{\dagger}_{ox}} = \gamma_0\,(1-\rho) + \gamma\,\rho \tag{7}$$

and

$$\varepsilon^{\dagger}_{nadp} = \frac{\varepsilon^{\dagger}_{CO_2}}{\nu^{\dagger}_{nadp}} = \frac{\alpha_0\,(1-\rho) + \alpha\,\rho}{\gamma_0\,(1-\rho) + \gamma\,\rho} \tag{8}$$

For native photorespiration, glycerate, all carbon-neutral and tartronyl-CoA shunts $\varepsilon^{\dagger}_{nadp} = 0.31$, 0.36, 0.38 and 0.40. The synthetic shunts are 14, 20 and 28% more NADPH efficient than native photorespiration. In summary the consumer model shows that we can expect the synthetic shunts operating alongside the Calvin Cyle to be more energy and carbon efficient than native photorespiration/photosynthesis. Moreover, the carbon-neutral and carbon-fixing shunts are also more efficient than the glycerate shunt.

Rubisco kinetics

In all of the following, we assume that Rubisco is always saturated with RuBP and that the concentration of RuBP exceeds the concentration of Rubisco. Then

$$v^{\dagger}_{carb} = v_{carb\_max}\,\frac{x}{x + k_3} \tag{9}$$

$$v_{ox}^{\dagger} = v_{ox\_max} \frac{k_2}{x + k_3} \tag{10}$$

with the following definition for k_2 and k_3:

$$k_2 = k_c \frac{O}{k_o} \tag{11}$$

$$k_3 = k_c \left(1 + \frac{O}{k_o}\right) \tag{12}$$

The concentration of CO_2 at the site of carboxylation in the stroma (C_c), is here given the symbol x.

The parametrisation of Rubisco's carboxylase ($v_{carb}^{\dagger}$) and oxygenase ($v_{ox}^{\dagger}$) rates in the consumer model is as follows: k_c and k_o are the Michaelis constants for CO_2 and O_2 respectively, v_{carb_max} and v_{ox_max} are the maximal rates of carboxylase and oxygenase respectively. O is chloroplast O_2 concentration and is assumed to be constant. It is calculated with Henri's law at atmospheric oxygen partial pressure (see Section 3.1.4).

Since $v_{carb}^{\dagger}$ and $v_{ox}^{\dagger}$ have the same denominator, it is possible to express one in terms of the other.

$$v_{ox}^{\dagger} = v_{ox\_max} \frac{k_2}{x + k_3} \cdot \frac{v_{carb\_max} \cdot x}{v_{carb\_max} \cdot x} = v_{carb\_max} \frac{x}{x + k_3} \cdot \frac{v_{ox\_max} \cdot k_2}{v_{carb\_max} \cdot x} = v_{carb}^{\dagger} \cdot (\Lambda / x) \tag{13}$$

with

$$\Lambda = \frac{v_{ox\_max}}{v_{carb\_max}} k_2 = \frac{v_{ox\_max}}{v_{carb\_max}} \frac{k_c}{k_o} O \tag{14}$$

The † superscript indicates that we are still referring to the consumer model of photosynthesis.

3.1.3 Stoichiometric-kinetic model

We now extend the consumer model to a full steady state model that also takes the supply of CO_2, ATP and NADPH into account. At steady-state, for all three of these, the supply must equal the demand (consumption). This model is in many features very similar to the Farquhar, von Caemmerer and Berry (FvCB) model [1] that has been the cornerstone of most photosynthetic models in the past 30 years. However, we extend and generalise the model, both to our new synthetic shunts and to previously neglected limitations, namely limitations by the enzymatic activities of Calvin Cyle and photorespiration enzymes.

The overall carbon fixation rate A is a function of the environmentally controlled variables light irradiance (I) and intercellular carbon dioxide concentration (C_i). The latter is the CO_2 concentration in the intercellular airspaces inside the leaf that are connected to the outside via stomata (pores) on the leaf's surface. CO_2 diffuses from the atmosphere into intercellular airspaces and from there into

the photosynthetic (mesophyll) cells. Plants can regulate the amount of CO_2 that diffuses into the intercellular airspaces (which is correlated to water loss) according to their needs (which can change with e.g. temperature and water status), by opening or closing their stomata. Thus, intercellular CO_2 concentration can vary considerably. At any given combination of I and C_i, A can be described as the minimum of six rates (we ignore limitation by product removal since this only occurs at very high carbon concentrations, well above physiological levels):

$$A = \min\{A_{rbc},\, A_{atp},\, A_{nadp},\, A_{cbb},\, A_{pr},\, A_{cbx}\} \tag{15}$$

The carbon fixation rate is either limited by Rubisco (A_{rbc}), light, or a second enzyme in either the Calvin Cyle, native photorespiration or the shunt replacing native photorespiration. Light limits both NADPH (A_{nadp}) and ATP (A_{atp}) production and in different circumstances one or the other can become limiting. As to a second limiting enzyme, we differentiate between enzymes in the Calvin Cyle proper (A_{cbb}) or in native photorespiration / a photorespiration shunt (A_{pr}). Moreover, when a second carboxylating enzyme is present, as in the carbon-fixing shunt, we treat this enzyme separately (A_{cbx}) because its rate, unlike the others, depends on the concentration of CO_2 in the chloroplast.

In contrast to the FvCB model [1, 3], which is routinely applied to experimental data on photosynthesis, we prefer a 'bottom-up' approach, i.e. we determine chloroplast CO_2 concentration from quadratic equations and A is then calculated from the diffusion equation (Eq. 16; in the FvCB model this sequence is reversed). Since chloroplast CO_2 (C_c) has such a central role in our models we give it the symbol x.

$$\begin{aligned} A &= g_i\,(C_i - x) \\ x &= \max\{x_{rbc},\, x_{atp},\, x_{nadp},\, x_{cbb},\, x_{pr},\, x_{cbx}\} \end{aligned} \tag{16}$$

We omit the day respiration rate from our description since it only adds an offset to the apparent C_i. The indices of x have the same meaning as for A. In each case it implies a steady state where only the corresponding limitation is in force.

What is not explicitly stated in Eq. 15 is that CO_2 diffusion itself is co-limiting no matter what other limitation we impose because we will never assume (except earlier in the consumer model) that CO_2 supply is unlimited. This is the consequence of the finite and limiting value of g_i (in relation to v_{carb_max}) which is small enough to lead to a non-negligible difference between C_i and x, and x needs to be positive. Therefore, in the following, any specific limitation defined in Eq. 15 by implication also means CO_2 diffusion co-limitation.

Calculating steady-state chloroplast CO_2 concentration

At steady state, CO_2 diffusion into the chloroplast has to be equal to CO_2 fixation in the chloroplast.

$$A = g_i\,(C_i - x) = v_{carb} + \alpha\, v_{ox} \tag{17}$$

Equally,

$$v_{carb} = v_{ox} \cdot (x/\Lambda) \tag{18}$$

and the fundamental diffusion equation (Eq. 17) can be succinctly written as

$$A = g_i\,(C_i - x) = v_{carb}\,(1 + \alpha\,\Lambda/x) \tag{19}$$

or

$$A = g_i\,(C_i - x) = v_{ox}\,(x/\Lambda + \alpha) \tag{20}$$

Rubisco rate parametrisation

We have been careful to distinguish between A and $A^\dagger$, and also between v_{carb}, v_{ox} and its counterparts $v^\dagger_{carb}$, $v^\dagger_{ox}$, indicating either the supply-demand (no superscript) or the consumer model (with †) respectively. The reason we do this is to address a problem that becomes apparent if one expresses the steady-state model in terms of x, the chloroplast CO_2 concentration, and not in terms of A, as in the FvCB model. If we solve Eq. 17 assuming $v_{carb} = v^\dagger_{carb}$ and $v_{ox} = v^\dagger_{ox}$, i.e. the Rubisco parametrisation introduced earlier (Eqs 9 and 10)), we obtain a single solution for $x = x_{rbc}$ and fixed values of g_i and C_i as well as Rubisco kinetic constants. This implies that there can be no other steady state than $x = x_{rbc}$ if none of of these parameters change. On the other it is clear that other steady states must exist, e.g. when light is limiting. The FvCB model does not propose that the aforementioned parameters change (this is a justifiable simplification), and as a matter of fact it does not explain how other steady states are possible that simultaneously fullfil the diffusion equation Eq. 17 and the Rubisco rate equations Eq. 9 and 10. The conundrum is hidden rather than resolved in the FvCB model. The focus on A instead of x avoids the issue we describe here.

We, too, do not propose that parameters such as g_i and C_i need to change to make other steady states possible. Rather, we introduce a new parameter, the attenuation factor τ that scales down both the oxygenase and carboxylase activity of Rubisco such that steady states at lower carbon fixation rates (e.g. light limitation) become feasible. This can be easily understood as the down-regulation, inhibition or inactivation of Rubisco at low light. From this perspective, τ is the proportion of active enzyme remaining. Thus we define the oxygenase and carboxylase rate as

$$v_{carb} = \tau \cdot v_{carb\_max}\,\frac{x}{x + k_3} = \tau \cdot v^\dagger_{carb} \tag{21}$$

$$v_{ox} = \tau \cdot v_{ox\_max}\,\frac{k_2}{x + k_3} = \tau \cdot v^\dagger_{ox} \tag{22}$$

and

$$\begin{aligned} \tau &= \frac{A}{A^\dagger} = \frac{g_i\,(C_i - x)}{v^\dagger_{carb} + \alpha \cdot v^\dagger_{ox}} \\ &= \frac{g_i\,(C_i - x)}{v_{carb\_max}\,\frac{x+\alpha\,\Lambda}{x+k_3}} \\ 0 &\le \tau \le 1 \end{aligned} \tag{23}$$

The introduction of τ makes steady states at net carbon fixation rates less than $A^\dagger$ possible. Importantly, this is not the frivolous introduction of a new parameter, but rather the necessary amendment of the FvCB model in which the light limited chloroplast CO_2 concentration cannot simultaneously fulfil the diffusion and the Rubisco rate equations. Far from constituting an additional degree of freedom, the the new parameter τ is fully determined in every limitation that the FvCB model deals with, as we shall see in the following. For each limitation there is a (x, τ) pair that fulfils all the equations.

Rubisco limited rate A_{rbc}

To begin with, we look at the situation where Rubisco is limiting. By this we mean the situation where there is unlimited supply of NADPH and ATP (e.g. at saturating light) and no other enzyme that is limiting. Therefore the steady state is a trade-off between CO_2 diffusion (supply) and Rubisco-dependent carbon fixation (demand) only. We assume under these conditions that Rubisco is fully activated i.e. $\tau = 1$ and $A = A^\dagger$. With the definitions of Eqs 17, 21, and 22, we obtain

$$\begin{aligned} A_{rbc} = g_i\,(C_i - x_{rbc}) &= \tau \cdot v_{carb\_max}\,\frac{x_{rbc}}{x_{rbc}+k_3} + \tau\cdot\alpha\, v_{ox\_max}\,\frac{k_2}{x_{rbc}+k_3} \\ &= v_{carb\_max}\,\frac{x_{rbc}}{x_{rbc}+k_3} + \alpha\, v_{ox\_max}\,\frac{k_2}{x_{rbc}+k_3} \\ &= v_{carb\_max}\,\frac{x_{rbc}+\alpha\,\Lambda}{x_{rbc}+k_3} \end{aligned} \tag{24}$$

After rearranging Eq. 24 we obtain a quadratic equation that has a single positive solution (assuming all parameters other than x are fixed). In other words, the value $x = x_{rbc}$ is the only (positive) value of x that fulfils the above equation given that $\tau = 1$. The generic solution is

$$x = \frac{-b + \sqrt{b^2 - 4ac}}{2a} \tag{25}$$

with the following coefficients when solving for x_{rbc}.

$$\begin{aligned} a &= 1 \\ b &= \frac{v_{carb\_max}}{g_i} + k_3 - C_i \\ c &= \alpha\,\frac{v_{carb\_max}\,\Lambda}{g_i} - C_i\,k_3 \end{aligned} \tag{26}$$

The rate A_{rbc} is then calculated by substituting x_{rbc} into Eq. 17.

NADPH limitation

Light irradiance (I) is converted to electron flux (J) and this in turn is used to generate ATP and NADPH. The equations for the first part of this process [4], i.e. conversion of I to J, are described in the Section 3.1.4.

We now make the assumption that when NADPH is limiting a stoichiometric amount of NADPH is made from the available electron flux J, i.e. that the rate of supply of NADPH equals $J/2$ (two electrons make one NADPH). Since we know how many NADPHs are needed to sustain one turn of the Calvin Cyle (i.e. $\gamma_0 = 2$) and equally how many NADPHs are needed for one turn of a photorespiration cycle (depending on the pathway, e.g. $\gamma = 2$ in native photorespiration), we can calculate the rate of demand for NADPH as a function of v_{ox} and v_{carb}. In this manner we obtain a relationship between the light-dependent supply and the Rubisco-dependent demand for NADPH.

$$0.5\,J = \gamma_0\,v_{carb} + \gamma\,v_{ox} = v_{carb}\,(\gamma_0 + \gamma\,\Lambda/x_{nadp}) \tag{27}$$

On the left side of the equation we have the supply of NADPH. The factor of 0.5 reflects that two electrons are needed for the production of one NADPH. On the right side of the equation, the demand for NADPH is expressed in terms of the flux through the carboxylating and oxygenating cycle. $\gamma_0 = 2$ is the number of NADPHs consumed in the Calvin Cyle and γ is the number NADPHs consumed in the photorespiration shunt.

Next, we arrange Eq. 27, such that we can substitute v_{carb} with an expression containing only J, x_{nadp} and fixed parameters.

$$v_{carb} = 0.5\,J\,\frac{x_{nadp}}{\gamma_0\,x_{nadp} + \gamma\,\Lambda} \tag{28}$$

Clearly there is an upper limit of v_{carb} that can be expressed in terms of J:

$$\lim_{x_{nadp}\to\infty} v_{carb} = \frac{0.5\,J}{\gamma_0} = \frac{J}{4} \tag{29}$$

On substituting Eq. 28 into the diffusion equation (Eq. 17), we obtain

$$\begin{aligned} A_{nadp} = g_i\,(C_i - x_{nadp}) &= v_{carb} + \alpha\cdot v_{ox} \\ &= v_{carb}\cdot(1 + \alpha/x_{nadp}) \\ &= 0.5\,J\,\frac{x_{nadp}}{\gamma_0\,x_{nadp} + \gamma\,\Lambda}\cdot(1 + \alpha/x_{nadp}) \\ &= 0.5\,J\,\frac{x_{nadp} + \alpha\,\Lambda}{\gamma_0\,x_{nadp} + \gamma\,\Lambda} \\ &= \frac{J}{2\,\gamma_0}\cdot\frac{x_{nadp} + \alpha\,\Lambda}{x_{nadp} + \frac{\gamma}{\gamma_0}\,\Lambda} \end{aligned} \tag{30}$$

The similarities to Eq. 24 are evident. This also leads to a quadratic equation in x_{nadp} with the generic solution given in Eq. 25. Here the coefficients are

$$\begin{aligned} a &= \gamma_0 \\ b &= \frac{0.5\,J}{g_i} + \gamma\,\Lambda - \gamma_0\,C_i \\ c &= \alpha\,\frac{0.5\,J\,\Lambda}{g_i} - C_i\,\gamma\,\Lambda \end{aligned} \tag{31}$$

The rearrangement of Eq. 27 and the subsequent substitution of v_{carb} (Eq. 30), which is analogously done in the FvCB model, effectively makes τ disappear: The final equation does no longer contain the maximal rates of Rubisco, be they scaled by τ or not. That is why our model, with τ, is equivalent to FvCB without τ. However, our model allows us to back-substitute the steady-state solution x_{nadp} into the first line of Eq. 30 and then use the definition of Eq. 21 and 22:

$$\begin{aligned} A_{nadp} = g_i\,(C_i - x_{nadp}) &= v_{carb} + \alpha \cdot v_{ox} \\ &= \tau \cdot v_{carb\_max}\,\frac{x_{nadp}}{x_{nadp} + k_3} + \alpha \cdot \tau \cdot v_{ox\_max}\,\frac{k_2}{x_{nadp} + k_3} \\ &= \tau \cdot v_{carb\_max}\,\frac{x_{nadp} + \alpha \cdot \Lambda}{x_{nadp} + k_3} \end{aligned} \tag{32}$$

Here is the point where the FvCB model breaks because it implies $\tau = 1$. The absurd conclusion would be that there is only a steady-state where $x_{nadp} = x_{rbc}$ and $A_{nadp} = A_{rbc}$.

The value of τ can be calculated with Eq. 22

$$\begin{aligned} \tau &= \frac{g_i\,(C_i - x_{nadp})}{v_{carb\_max}\,\frac{x_{nadp}+\alpha\,\Lambda}{x_{nadp}+k_3}} \\ &= \frac{0.5\,J\,\frac{x_{nadp}+\alpha\,\Lambda}{\gamma_0\,x_{nadp}+\gamma\,\Lambda}}{v_{carb\_max}\,\frac{x_{nadp}+\alpha\,\Lambda}{x_{nadp}+k_3}} \\ &= \frac{0.5\,J \cdot (x_{nadp} + k_3)}{v_{carb\_max} \cdot (\gamma_0\,x_{nadp} + \gamma\,\Lambda)} \end{aligned} \tag{33}$$

The amount of down-regulation of Rubisco that τ represents depends on γ but not on α. Since the carbon-neutral pathway and native photorespiration have the same γ, the amount of down-regulation represented in τ is the same. However, their NADPH-limited assimilation rates A_{nadp} are not the same because of the higher carbon efficiency of the carbon-neutral pathway.

ATP limitation

ATP limitation works in exactly the same way as NADPH limitation with two differences: β replaces γ and the number of ATP molecules per electron is 0.75 (we assume that per electron, 3 protons are pumped and that 4 protons are required to make one ATP), not 0.5. Thus

$$A_{atp} = g_i\,(C_i - x_{atp}) = 0.75\,J\,\frac{x_{atp} + \alpha\,\Lambda}{\beta_0\,x_{atp} + \beta\,\Lambda} \tag{34}$$

The solution to the quadratic is given in Eq. 25 with the coefficients

$$
\begin{aligned}
a &= \beta_0 \\
b &= \frac{0.75\,J}{g_i} + \beta\,\Lambda - \beta_0\,C_i \\
c &= \alpha\,\frac{0.75\,J\,\Lambda}{g_i} - C_i\,\beta\,\Lambda
\end{aligned}
\tag{35}
$$

The value of τ can be calculated with Eq. 22

$$
\begin{aligned}
\tau &= \frac{g_i\,(C_i - x_{atp})}{v_{carb\_max}\,\frac{x_{atp}+\alpha\,\Lambda}{x_{atp}+k_3}} \\
&= \frac{0.75\,J\cdot(x_{atp}+k_3)}{v_{carb\_max}\cdot(\beta_0\,x_{atp}+\beta\,\Lambda)}
\end{aligned}
\tag{36}
$$

Limitation by a Calvin Cyle enzyme

The FvCB model considers only a subset of the limitations of supply-demand model, namely limitation by Rubisco or light at physiological C_i. Since this model is ubiquitously applied we define the restricted supply-demanded model fixation rate explicitly as

$$
A^* = \min(A_{rbc},\, A_{nadp}, A_{atp}) \tag{37}
$$

As this definition shows, the FvCB model assumes that none of the Calvin Cyle enzymes other than Rubisco or light are limiting carbon assimilation. This may not always be the case. For example, it has been shown that the activity of sedoheptulose-bisphosphatase (SBPase) can be rate limiting [5]. SBPase, like all other Calvin Cyle enzymes, also participates in native photorespiration because the molecules of PGA that are the outcome of native photorespiration also need to be converted into RuBP. In general, the flux of a given Calvin Cyle enzyme v_{cbb} can be expressed as

$$
v_{cbb} = \eta_{ox}\,v_{ox} + \eta_{carb}\,v_{carb} \tag{38}
$$

The values of η_{ox} and η_{carb} depend entirely on the stoichiometry of the Calvin Cyle and photorespiration or the synthetic photorespiratory shunt replacing it. They can be read off Table 2. For many enzymes $\eta_{ox} = \eta_{carb}$.

Parametrisation of a Calvin Cyle enzyme

We parametrize v_{cbb} with reversible Michaelis-Menten kinetics adopting the decomposition of [6]. Here the definitions are given for a uni-uni reaction but they can be easily applied to more complex reaction schemes.

$$
v = v^+ \cdot \frac{S/K_s}{1 + S/K_s + P/K_p} \cdot (1 - \frac{P/S}{K'_{eq}}) \tag{39}
$$

	η_{carb}	η_{ox}				
Pathway	Calvin cycle	Native PR[a]	TrCoA	Ru1P	Ar5P	Eu	Xu
Phosphoglycerate kinase	2	1.5	2	1		
GAP DH	2	1.5	2	1		
Sink	1/3	−1/6	1/3	0		
TPI	2/3			1	0	1	1
Aldolase	2/3			0	0	1	1
FBPase	1/3			0	0	0	1
Transketolase	2/3			0	0	1	0
SBPase	1/3			0	0	1	0
Isomerase	1/3			0	0	1	0
Epimerase	2/3			0	0	0	1
Phosphoribulokinase	1			0	1	1	1

Table 2: Flux distribtion of the Calvin cycle and photorespiratory bypasses. The table gives the stoichiometric coefficent η for each enzyme. The table gives the stoichiometric coefficent η for each enzyme, that has to be multiplied with the respective base rates, v_{carb} and v_{ox}. The total flux through an enzyme is the superposition of the fluxes originating from RuBP oxygenase and carboxylase (Eq. 38). Note that all pathways that channel G2P back to PGA have the same coefficients below the sink. The reason for this is that the entire flux goes via the regenerative part of the Calvin cycle. The carbon neutral shunts do not proceed in this manner, and there are differences within that group. The Ru1P and Ar5P shunts effectively bypass the majority of enzymes of the regenerative phase of the pentose phosphate cycle (i.e. their flux deriving from photorespiration is zero). Aldolase and transketolase catalyse two reactions each so their coefficient is the sum of the two reactions. Furthermore it is assumed that the Calvin cycle aldolase does not catalyse the aldolase reactions of the Ru1P and Ar5P shunts, but that transketolase does catalyse the transketolase reaction of the Eu shunt. [a] The values of η are the same for native photorespiration and the TSA shunt.

The three factors in this decomposition are the forward maximal rate , the fractional saturation and the thermodynamic driving force of the reaction. The maximal rate is defined by $v^+ = k_{cat}^+ \cdot E$, where E is the total concentration of enzyme and k_{cat}^+ is the maximal forward rate per unit of enzyme. S and P are the concentrations of substrate and product respectively, and K_s and K_p are their respective Michaelis constants. K'_{eq} is the ratio of P to S at equilibrium.

We now combine all three terms of Eq. 39 into a single parameter φ that combines saturation and driving force and expresses the maximal rate in units of the maximal carboxylase rate of Rubisco:

$$\varphi = \frac{v}{v_{carb\_max}} = \frac{v^+ \cdot \frac{S/K_s}{1+S/K_s+P/K_p} \cdot (1 - \frac{P/S}{K'_{eq}})}{v_{carb\_max}} \tag{40}$$

φ can be interpreted as the maximal rate scaled by the saturation of the enzyme and the thermodynamic driving force. expressed as a fraction of v_{carb_max}

Thus,

$$v_{cbb} = \varphi_{cbb} \cdot v_{carb\_max} \tag{41}$$

The advantage of this approach is that all the unknowns (in particular substrate concentrations) are condensed into a single scaling factor φ_{cbb}. Whenever the total activity of a Calvin Cyle enzyme is known (e.g. from the literature), it can be used to remove the effect of v^+.

Generic solution

The Calvin Cyle enzyme limited carbon-fixation rate can be found by expressing v_{ox} in terms of v_{cbb} and substituting this result into a diffusion equation that is also expressed in terms of v_{ox} (of course we could have used v_{carb} instead of v_{ox} in both cases). We are using the transformation $v_{carb} = v_{ox} \cdot x/\Lambda$.

$$\begin{aligned} v_{cbb} = \eta_{ox}\, v_{ox} + \eta_{carb}\, v_{carb} = v_{ox}\,(\eta_{ox} + \eta_{carb} \cdot x_{cbb}/\Lambda) \\ \Leftrightarrow\ v_{ox} = \frac{v_{cbb}}{\eta_{ox} + \eta_{carb} \cdot x_{cbb}/\Lambda} \end{aligned} \tag{42}$$

In the rearranged diffusion equation A is expressed in terms of v_{ox}:

$$A_{cbb} = g_i\,(C_i - x_{cbb}) = v_{carb} + \alpha\, v_{ox} = v_{ox} \cdot (x_{cbb}/\Lambda + \alpha) \tag{43}$$

Combining these two equation yields

$$A_{cbb} = g_i\,(C_i - x_{cbb}) = v_{cbb}\,\frac{x_{cbb}/\Lambda + \alpha}{\eta_{ox} + \eta_{carb} \cdot x_{cbb}/\Lambda} = v_{cbb}\,\frac{x_{cbb} + \alpha \cdot \Lambda}{\eta_{carb} \cdot\ x_{cbb} + \eta_{ox} \cdot \Lambda} \tag{44}$$

which is a quadratic in x_{cbb}. The only positive root is defined by the coefficients

$$\begin{aligned} a &= \eta_{carb} \\ b &= v_{cbb}/g_i + \eta_{ox} \cdot \Lambda - \eta_{carb} \cdot C_i \\ c &= \Lambda \cdot (\alpha \cdot v_{cbb}/g_i - \eta_{ox} \cdot C_i) \end{aligned} \tag{45}$$

Native photorespiration

On examination of Table 2, one observes that η_{ox} is equal to η_{carb} for a large subset of Calvin Cyle enzymes in native photorespiration and for all Calvin Cyle enzymes in the tartronyl-CoA pathway (but not in the carbon-neutral shunts). The subset of enzymes in native photorespiration consists of all enzymes beyond GAP (where the sink is situated) and includes all enzymes that are known to be lowly expressed, i.e. SBPase, FBPase, transketolase and aldolase [7, 8]. With this in mind, we can afford to ignore the general case $\eta_{ox} \neq \eta_{carb}$. Instead, for these two pathways we set $\eta_{ox} = \eta_{carb}$:

$$A_{cbb} = g_i\,(C_i - x_{cbb}) = v_{cbb}\,\frac{x_{cbb} + \alpha \cdot \Lambda}{\eta_{carb} \cdot\ x_{cbb} + \eta_{carb} \cdot \Lambda} = \frac{v_{cbb}}{\eta_{carb}} \cdot \frac{x_{cbb} + \alpha \cdot \Lambda}{x_{cbb} + \Lambda} \tag{46}$$

If $\alpha = -0.5$ as in native photorespiration, this is again a quadratic and the solution is given in Eq. 45.

Tatronyl-CoA shunt

However when $\alpha = 1$, the second fraction of Eq. 46 is equal to one and the solution is

$$A_{cbb} = v_{cbb}/\eta_{carb} \tag{47}$$

Therefore, in the tartronyl-CoA pathway, the rate of carbon fixation when a Calvin Cyle enzymes is limiting takes on a very simple form (Eq. 47) that is not dependent on C_i, i.e. it is always the same no matter what the CO_2 concentrations inside and outside the chloroplast are. In contrast, the rate of fixation of native photorespiration (Eq. 44) depends on the CO_2 concentrations x_{cbb} and C_i. The fixation rate A is proportional to the fraction $\frac{\Lambda+\alpha\, x_{cbb}}{\Lambda+x_{cbb}} < 1$ for any positive value of x_{cbb} and $\alpha = -0.5$. Thus, the carbon-fixing shunt always achieves a higher fixation rate A than native photorespiration at a fixed but limiting rate v_{cbb}.

The Ru1P/Ar5P carbon-neutral shunts

Here, Table 2 tells us that η_{ox} is not equal to η_{carb} for all enzymes. However, these carbon-neutral shunts redirects all flux resulting from photorespiration away from the regenerative part of the pentose phosphate pathway; η_{ox} is zero for all Calvin Cyle enzymes situated between the triose phosphates and Ru5P/RuBP. For these enzymes that, as stated earlier, are the ones most likely to be limiting in vivo, we arrive at a much simpler version of Eq. 44: if we substitute $\alpha = 0$ (carbon-neutral shunts) and $\eta_{ox} = 0$, we arrive at

$$A_{cbb} = g_i\,(C_i - x_{cbb}) = v_{cbb}\,\frac{x_{cbb} + 0\cdot\Lambda}{\eta_{carb}\cdot x_{cbb} + 0\cdot\Lambda} = v_{cbb}/\eta_{carb} \tag{48}$$

This is the same result we obtained for the carbon-fixing shunt. By the same token, the limitation by a Calvin Cyle enzyme in these carbon-neutral shunts is also independent of CO_2 concentrations and always higher than native photorespiration at a fixed and limiting value of v_{cbb}.

The Erythrulose/Xylulose carbon-neutral shunts

These pathways have have several things in common: flux through aldolase and one of the bisphosphatases (FBPase and SBPase). This is a case for the generic equation (Eq. 45).

Limitation by a photorespiration shunt enzyme

The argument for a photorespiration shunt enzyme is analogous to the previous section.

First we observe that v_{pr}, the flux a photorespiration enzyme has to carry, is equal to v_{ox} in all synthetic shunts.

In the tartronyl-CoA pathway, photorespiratory enzymes operate between phosphoglycolate and phosphoglycerate. Since the pathway is linear, it is easy to see that the flux at each step has to be equal

to v_{ox}. In contrast, in the arabinose-5P pathway, 2PG is first converted to glycolaldehyde (GA) in a linear chain of reactions. The flux has to be equal to v_{ox}. In the next step, GA is stoichiometrically combined with GAP (which is produced by Calvin Cyle enzymes); the rate again has to be equal to v_{ox} if GA is to be produced and consumed at the same rate (i.e. at steady state). The amount of GAP that is produced from every RuBP oxygenase reaction is also equal to v_{ox}. The remainder of the pathway is linear, and has to be equal to v_{ox} (Table 2). Therefore the rate of every enzyme of the arabinose-5P pathway has to be equal to v_{ox}. The argument would be analogous for the other carbon-neutral shunts described in the main text.

Native photorespiration is more complicated: it is linear in character, however, the flux stoichiometry changes from 1 to 0.5 times the flux of v_{ox} at the decarboxylation step that is carried out by the glycine cleavage complex. Therefore we define

$$v_{pr} = \epsilon \cdot v_{ox} \tag{49}$$

where ϵ is always equal to one for all synthetic shunts, also equal to one for all enzymes in native photorespiration leading up to the decarboxylation reaction and 0.5 thereafter (and also the transaminases and the ammonia refixation reactions). To be conservative, i.e. to assume the conditions that are most favourable to native photorespiration and the glycerate shunt, we can simply use $\epsilon = 0.5$, so requirements for a photorespiration enzyme are only half that for an enzyme in a synthetic shunt.

Next we parametrise this enzyme with reversible Michealis-Menten kinetics and simplify by introducing the scaling factor φ_{pr} in the same manner as we did for the Calvin Cyle enzyme (Eq.41).

$$v_{pr} = \varphi_{pr} \cdot v_{carb\_max} \tag{50}$$

We combine the rearranged diffusion equation (Eq. 43) with results from the previous two equations:

$$\begin{aligned} A_{pr} = g_i \left(C_i - x_{pr}\right) &= v_{ox} \left(x_{pr}/\Lambda + \alpha\right) \\ &= v_{pr}/\epsilon \cdot \left(x_{pr}/\Lambda + \alpha\right) \\ &= \varphi_{pr} \cdot v_{carb\_max} \cdot \left(x_{pr}/\Lambda + \alpha\right)/\epsilon \end{aligned} \tag{51}$$

Solving for x_{pr} yields

$$x_{pr} = \frac{C_i - \alpha \frac{\varphi_{pr} \cdot v_{carb\_max}}{\epsilon\, g_i}}{1 + \frac{\varphi_{pr} \cdot v_{carb\_max}}{\epsilon\, g_i\, \Lambda}} \tag{52}$$

Limitation by a photorespiratory shunt enzyme that is a carboxylase

We now investigate the more difficult case where the photorespiration shunt enzyme is a carboxylase, and hence its rate will depend on x directly. The argument is very similar to a non-carboxylating enzyme therefore we can use Eq. 49 without modification except that we call the rate of the carboxylating enzyme v_{cbx} and not v_{pr}. The reaction it catalysis is

$$S + CO_2 \rightarrow P \tag{53}$$

The difference appears in the parametrisation of the kinetic rate v_{cbx}:

$$v_{cbx} = v_{cbx\_max} \frac{x}{x + K_{cbx}} \cdot \frac{S}{S + K_M} = \varphi_{cbx}\, v_{carb\_max} \frac{x}{x + K_{cbx}} \tag{54}$$

As in the previous section, φ_{pr} is a scaling factor expressed in units of v_{carb_max} that include the saturation with all substrates other than CO_2, in this case the acceptor molecule of the carboxylation reaction. v_{cbx_max} is the maximal rate. K_{cbx} is the apparent Michaelis constant for CO_2. When the substrate of the carboxylase is HCO_3^-, we calculate K_{cbx} based on the assumption that CO_2 is in equilibrium with HCO_3^- due to the activity of carbonic anhydrase in the chloroplast. The carboxylation enzyme in the tartronyl-CoA pathway is indeed HCO_3^--dependent. The K_M of a typical carboxylases for HCO_3^- is in the range of $1\,mM$ [9]. Since the equilibrium constant for the hydration of carbon dioxide is about 100 in favour of HCO_3^- we arrive at $K_{cbx} = 1\,mM/100 = 10\,\mu M$ at a pH of 8.0 and an ionic strength of 0.25 which are the conditions in the stroma of the chloroplast (see Section 3.1.4).

Finally, we substitute Eq. 54 into the rearranged diffusion equation (Eq. 43). We also set $\alpha = 1$ since this only applies to the carbon-fixing shunt.

$$\begin{aligned} A_{cbx} = g_i\,(C_i - x) &= v_{ox}\,(x/\Lambda + 1) \\ &= v_{cbx}\ (x/\Lambda + 1) \\ &= \varphi_{cbx}\, v_{carb\_max}\,(x/\Lambda + 1)\,\frac{x}{x + K_{cbx}} \end{aligned} \tag{55}$$

The equation is again quadratic in x and the generic solution is given in Eq. 25 with the coefficients

$$\begin{aligned} a &= 1 + \frac{\varphi_{cbx}\, v_{carb\_max}}{g_i\,\Lambda} \\ b &= \alpha\,\frac{\varphi_{cbx}\, v_{carb\_max}}{g_i} + K_{cbx} - C_i \\ c &= -C_i\,K_{cbx} \end{aligned} \tag{56}$$

3.1.4 Physicochemical parameters

Henri's law

The solubility of a gas like CO_2 or O_2 in water is given by Henri's law [10]

$$c_{aq} = p_{gas} \cdot k_H \tag{57}$$

where c_{aq} is the molar concentration of the gas in solution, p_{gas} is the partial pressure of the gas and k_H is Henri's constant. For CO_2, $k_H = 0.034\ M\ (atm)^{-1}$ at $25\,^\circ\,C$ (298.15 K). The partial pressure of CO_2 in the intercellular airspace when the stomate are open is about 220 ppm [11], therefore the

equivalent concentration of CO_2 in water at $25\,^\circ C$ is 7.5 μM. The temperature dependence of k_H can be expressed in the form of the van't Hoff equation [10]:

$$k_H(T) = k_H(T_{ref}) \cdot e^{C \cdot (\frac{1}{T} - \frac{1}{T_{ref}})} \tag{58}$$

The constant $C = 2400\,K$ for CO_2; T is absolute temperature and T_{ref} is the reference temperature, 298.15 K. For example, at $30\,^\circ C$, k_H is 12% lower than at $25\,^\circ C$.

For O_2, Henri's constant is $k_H = 0.0013\,M\ (atm)^{-1}$ and the temperature dependency is $C = 1700\,K$.

The equilibrium constant and steady state concentration of HCO_3^-

It is assumed that the concentration of aqueous CO_2 (representing both the species of $CO_2(aq)$ and H_2CO_3) is in equilibrium with the gaseous phase (see Henri's law). Furthermore, dissolved CO_2 is assumed to be in equilibrium with HCO_3^- by the action of carbonic anhydrase. Then the concentration of HCO_3^- is given by

$$HCO_3^- = K_{eq} \cdot CO_2 \tag{59}$$

where K_{eq} is the equilibrium constant of the combined hydration and dissociation reaction

$$CO_2 + H_2O \rightleftharpoons HCO_3^- + H^+ \tag{60}$$

K_{eq} is often expressed on the log scale as a pK_a,

$$K_{eq} = 10^{-pK_a} \Leftrightarrow pK_a = -log_{10}(K_{eq}) \tag{61}$$

so that the well-known Henderson-Hasselbach [12] equation can be applied to find the concentration of HCO_3^- when pH, the pK_a and the concentration of CO_2 are known.

$$pH = pK_a + log_{10}\frac{HCO_3^-}{CO_2} \Leftrightarrow\ HCO_3^- = CO_2 \cdot 10^{pH - pK_a} \tag{62}$$

Calculating the pK_a

The pK_a for Eq. 60 is often over- or underestimated because it is either measured in pure water or seawater, while the chloroplast has a salinity and ionic strength between pure water and saltwater.

Empirical formulae for this pK_a have been developed, depending on (absolute) temperature T and salinity S. According to Roy et al.[13] the $ln(K_{eq})$ (not the decadic logarithm) is calculated with:

$$ln(K_{eq}) = a_1 + \frac{a_2}{T} + a_3\, ln(T) + (b_1 + \frac{b_2}{T})\, S^{0.5} + c\, S + d\, S^{1.5} \tag{63}$$

With the parameters

$$\begin{aligned} a_1 &= 2.83655 \\ a_2 &= -2307.1266 \\ a_3 &= -1.5529413 \\ b_1 &= -0.20760841 \\ b_2 &= -4.0484 \\ c &= 0.08468345 \\ d &= -.00654208 \end{aligned} \tag{64}$$

The pK_a on the more common negative decadic logarithm scale is

$$pK_a = log_{10}(exp(ln(K_{eq}))) \tag{65}$$

Salinity and ionic strength

The above formulae have been developed for and applied to seawater where salinity is well-defined. The term has some correspondence to the ionic strength (I) of intracellular fluids, however, since both salinity and ionic strength depend on the composition of the 'salts' in solution, again an empirical conversion has to be used [14]:

$$I = \frac{19.92\, S}{1 + 1.005\, S} \;\Leftrightarrow\; S = \frac{I}{19.92 + 1.005\, I} \tag{66}$$

Calculation of K_{eq} in the chloroplast

We assume that the pH in the chloroplast is 8.0 [15] and that ionic strength is 0.25 [16]. The latter corresponds to a salinity of 0.14 (roughly 40% of the salinity of seawater, Eq. 61). Applying Eq. 64, we obtain a pK_a of 5.98. Since there are close to two pH units between the pK_a and the pH, the equilibrium contant is $K_{eq} = 10^2 = 100$. This is the value we use in our calculations.

Mathematical model of the light reactions

The light reactions are modelled by the empirical equation [17]

$$J = \frac{I_2 + J_{max} - \sqrt{(I_2 + J_{max})^2 - 4\,\theta\, J_{max}\, I_2}}{2\,\theta} \tag{67}$$

where

$$I_2 = \frac{a\,(1-f)}{2} \cdot I \tag{68}$$

I_2 is the amount of light photosystem II absorbs; $a = 0.85$ is the absorptance of leaves, $f = 0.15$ is a correction for spectral quality. The denominator of two is a consequence of each photosystem absorbing half of the light. I is irradiance and $\theta = 0.7$ is a curvature factor (values taken from [3]. J_{max} is the maximal electron flux.

Light limitation

When light is limiting, the model is either ATP or NADPH limited (Eq. 34 and Eq. 30 respectively). However, at steady state the correct amounts of both ATP and NADPH that are dictated by the stoichiometry of the Calvin Cyle and photorespiration need to be produced. We take the approach that we assume that the amount of ATP that is produced is limiting, and that the excess of NADPH that would produced by linear electron flow at the required electron flux for ATP production is by some mechanism corrected to the necessary stoichiometric amount. It has been shown that in this scenario, the maximal capacity of the electron chain can be extrapolated by calculating $J_{max} = 2.3 \cdot v_{carb\_max}$ [18]. Conversely, we could have used the approach that assumes that NADPH is limiting, in which case the ratio of J_{max} to v_{carb_max} would be close to 2.0. Both approaches give very similar results.

Carbon dioxide transfer conductances

We only use a single conductance because our synthetic pathways and the glycerate shunt are contained in a single compartment, the chloroplast. Including more conductances into the model would only affect native photorespiration, and in a negative manner. By using a single conductance we are being conservative in the sense that native photorespiration is described as being 100% efficient in recycling photorespiratory CO_2 from mitochondria to chloroplasts, which is unrealistic. As von Caemmerer and colleagues have shown, several conductances/resistances can be modelled, resulting in a worse performance of native photorespiration with respect to the glycerate shunt [3].

3.2 Results

In this Section, we will put the methodology that we established in the previous one into practice. To this end we need to put some actual numbers on the kinetics constants of Rubisco's rate equation and carbon dioxide diffusion that are representative of C3 photosynthesis.

3.2.1 Parameters and variables

The parameters listed in Table 3 are mostly identical to the ones von Caemmerer and colleagues have used in numerous publications [19, 17]. All partial pressures have been converted to molar concentrations. We note that the maximal carboxylation rate is close to four times the maximal oxygenation rate. The units of the rates are $\mu mole\ m^{-2}\ s^{-1}$, and the value of v_{carb_max} =80 $\mu mole\ m^{-2}\ s^{-1}$ corresponds to a k_{cat} of 3.5 s^{-1} and 2.3 mM Rubisco. The effective Michaelis constant for both the carboxylase

and oxygenase reactions, k_3, is 18.7 μM. The value of Λ, which is related to the carbon-compensation point [19] of native photorespiration ($\Gamma_* = 0.5\,\Lambda$) is 2.6 μM.

Name	Explanation	value	units
O	Chloroplast oxygen concentration	252	μM
x	Chloroplast CO_2 concentration	0 - 8	μM
C_i	Intercellular CO_2 concentration	2 - 8	μM
g_i	Transfer conductance	9.0	$\mu mole\, m^{-2}\, s^{-1}\, (\mu M)^{-1}$
v_{carb_max}	RuBP carboxylase V_{max}	80	$\mu mole\, m^{-2}\, s^{-1}$
k_c	Rubisco Michaelis constant for CO_2	8.6	μM
v_{ox_max}	RuBP oxygenase V_{max}	20	$\mu mole\, m^{-2}\, s^{-1}$
k_o	Rubisco Michaelis constant for O_2	215	μM
k_2	$k_2 = k_c\, O/k_o$	10.1	μM
k_3	$k_3 = k_c\,(1 + O/k_o)$	18.7	μM
Λ	$\Lambda = \frac{v_{ox\_max}\, k_c}{v_{carb\_max}\, k_o}\, O$	2.6	μM
I	Irradiance	200 - 1500	$\mu E\, m^{-2}\, s^{-1}$
v_{ox_max}/v_{carb_max}	Ratio of maximal velocities	0.255	
k_{cat}	Catalytic constant	3.5	s^{-1}

Table 3: Kinetic constants of Rubisco and CO_2 diffusion. The values are taken from [19, 17] and were converted from partial pressures in bar to molar concentrations. g_i is the transfer conductance of CO_2 from the intercellular airspace to the chloroplast.

Light irradiance and intercellular airspace CO_2 concentration are the key environmental variables that determine the carbon fixation rate A. We use a light range between 200 and 1500 $\mu E\, m^{-2}\, s^{-1}$ (from 'low' to 'high' light). The latter is considered 'saturating', in the sense that A levels off well before that point. However, light irradiance can be as high as 2000 on a clear day in central Europe [20]. The intercellular airspace CO_2 concentration C_i is the concentration of CO_2 inside the leaf but outside the photosynthetic cells. Since diffusion of CO_2 from the atmosphere into the leaf is correlated to diffusion of water vapour out of the leaf, there are experimental methods to estimate C_i [11]. Atmospheric CO_2 (partial pressure of 400 ppm) corresponds to a concentration of 13.6μM (Henri's law) and the C_i is considerably lower than that. Recently, careful measurements of C_i gave a value of about 220 ppm (7.5 μM) when the stomata were open and about 65 ppm (2.2 μM) when the stomata were closed [11]. Therefore, to cover the full range of physiologically possible values, we use a 'high' C_i value of 8 μM and a 'low' C_i value of C_i =2 μM.

The CO_2 transfer conductance from intercellular airspace to chloroplast (g_i) is also central to our model. We use a value of 9 $\mu mole\, m^{-2}\, s^{-1}\, \mu mole^{-1}$ which corresponds to 0.3 $\mu mole\, m^{-2}\, s^{-1}\, \mu bar^{-1}$, which is in the middle of the range that has been measured in plants [17]. A recent microscale simulation of photosynthesis also arrived at the same value of g_i [21].

3.2.2 Rubisco kinetics

The two equations that govern the carboxylase and oxygenase activity of Rubisco are given in Section 3.1.3. On plugging in the numbers from our parameter set, we obtain two curves that show the dependence of these rates on the chloroplast CO_2 concentration x (Fig. 4A). The oxygenase activity, $v^{\dagger}_{ox}$ only depends on x indirectly, as a competitive inhibitor of its substrate O_2 (which is constant). Therefore the curve falls moderately but monotonically with increasing x. In contrast, the carboxylation rate $v^{\dagger}_{carb}$ displays apparent Michaelis-Menten kinetics with respect to x. The the † superscript indicates

the consumer model where x which determines ρ is a free variable. In the kinetic-stoichiometric model, x cannot be chosen freely but is fully determined by the limitations imposed on the model, e.g. CO_2 diffusion into the chloroplast. It monotonically increases with x. The apparent Michaelis constant k_3 =18.7 μM which takes into account competitive inhibition by O_2 is considerably higher than the upper limit of x ($x \leq C_i \leq 8\ \mu M$). Importantly, Rubisco is always sub-saturated with respect to CO_2, which limits its rate to less than 30 % of its nominal v_{max} (which is measured at saturating CO_2).

The net carbon fixation rate $A^\dagger$ is a linear combination of the rates $v^\dagger_{carb}$ and $v^\dagger_{ox}$. The contribution of $v^\dagger_{carb}$, i.e. the Calvin cycle, is always positive with respect to $A^\dagger$ (i.e. carbon-fixing) no matter which photorespiration pathway it is paired with. The contribution of $v^\dagger_{ox}$ can be negative (i.e. releasing CO_2, as in native photorespiration), neutral or positive. This is encapsulated in the parameter α of each pathway (Table 1). Fig. 4B graphically depicts the net fixation rates of the four photorespiration pathways when each is paired with the Calvin cycle. Each combination of photorespiration pathway with the Calvin cycle is a function of x, but since there is no interaction between the Calvin cycle and the photorespiration pathway or shunt, one can simply view the resulting carbon fixation rate $A^\dagger$ as a superposition of the two base rates $v^\dagger_{carb}$ and $v^\dagger_{ox}$: The carbon-fixing pathway paired with the Calvin cycle is the sum of the $v^\dagger_{carb}$ and $v^\dagger_{ox}$ and native photorespiration or glycerate shunt paired with the Calvin cycle correspond to $v^\dagger_{carb} - 0.5\, v^\dagger_{ox}$. A carbon-neutral shunt paired with the Calvin cycle is identical to $v^\dagger_{carb}$ since there is neither a positive nor a negative contribution from $v^\dagger_{ox}$.

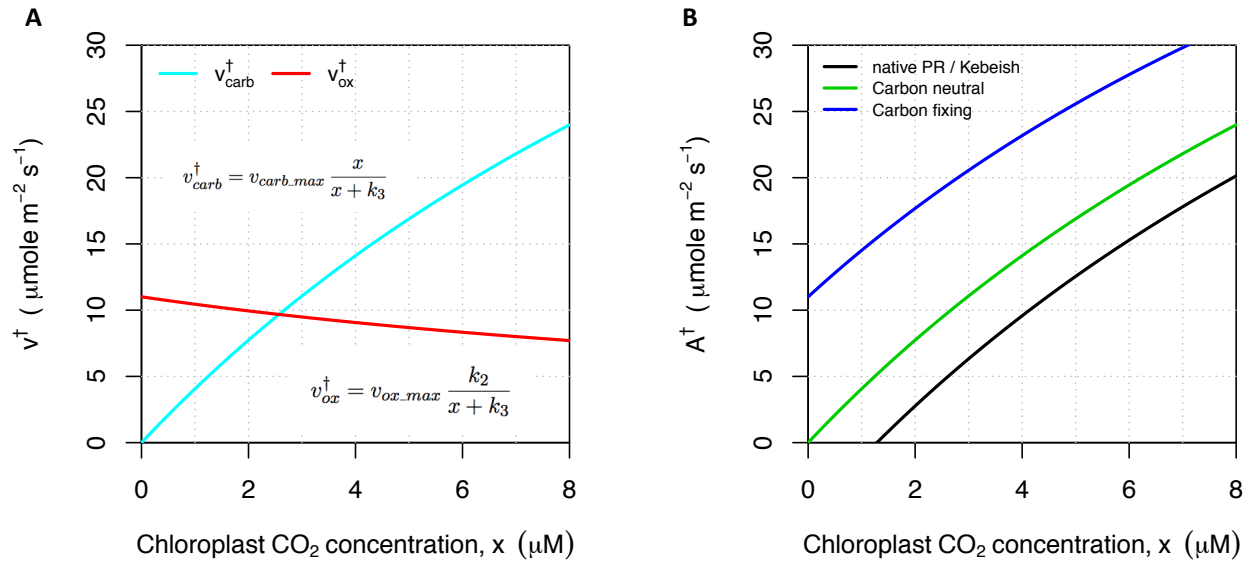

Figure 4: Rubisco kinetics and net carbon fixation rates in the consumer model. A: The rates of RuBP carboxylase ($v^\dagger_{carb}$, cyan) and RuBP oxygenase ($v^\dagger_{ox}$, red) are plotted as a function of chloroplast CO_2 concentration. The two rate equations are shown in the plot. B: Net carbon fixation rates of photosynthesis, i.e. the Calvin cycle paired with a photorespiration pathway as a function of chloroplast CO_2 concentration. The blue and green lines are the net fixation rates of the Calvin cycle paired with a carbon-fixing or a carbon-neutral shunts respectively (it applies equally to all four carbon-neutral shunts). Native photorespiration and Calvin cycle is shown as black line (the glycerate shunt gives identical results). The underlying assumption of the consumer model (Section 3.1.2) is that the rates are not limited by the supply of CO_2, ATP or NADPH. The kinetic parameters for these plots can be found in Table 3.

3.2.3 Limitation by light

The variable x is of central importance, as the curves in Fig 4 clearly show. The ratio of activities of either of our synthetic shunts to native photorespiration, i.e. the activity of a synthetic photorespiration shunt paired with the Calvin cycle expressed divided by the the activity of native photorespiration paired with the Calvin cycle [1] at the same x, is much bigger at low C_i than at high x. Unfortunately, x cannot be controlled in an experiment or even directly measured and has to be inferred, i.e. calculated from a model. The variables that can be manipulated are light irradiance and C_i. Therefore it is common practice to measure the response curves of the net carbon fixation rate with respect to light and C_i [17].

The restricted kinetic-stoichiometric model, which is equivalent to the FvCB model [17] calculates the carbon fixation rate A^* using the assumption that only light and Rubisco are limiting. We will also use this assumption for the present time, but we will later introduce additional factors that can limit A (see Section 3.2.4). The light response curve of the restricted kinetic-stoichiometric model (Fig. 5) has two readily distinguishable phases, first rising monotonically with increasing irradiance and then reaching a plateau. The two phases correspond to light limitation (here via ATP) and limitation by Rubisco. The amount of Rubisco and the available CO_2 that diffuses into the cell define the upper limit A_{rbc} above which it does not matter if additional energy in the form of ATP and NADPH becomes available.

The light response curve has a different appearance at low $C_i = 2\mu M$ (Fig. 5B) compared to high $C_i = 8\mu M$ (Fig. 5A): The curves reach the plateau much earlier. In other words, Rubisco becomes limiting much earlier and this is because at low C_i the contribution of v_{ox} is much more important than at high C_i. The effect is two-fold: first, for pathways with negative α (native photorespiration and glycerate shunt), v_{ox} is subtracted from v_{carb}. Second, in pathways where α is non-negative, the much lower absolute rate of v_{carb} leads to the largest decrease in the fixation rate. For example, in the carbon-fixing shunt, the two rates, v_{carb} and v_{ox} are added 1:1. One may naively expect that in these circumstances the loss in v_{carb} might be compensated by the increase in v_{ox}. This is not the case: the maximal rate of v_{carb} is four times higher than v_{ox}, and also the fall in its activity is much sharper at low C_i than the corresponding rise in v_{ox}.

The differences between the different photorespiration pathways is immediately visible in their light response curves. The carbon-neutral shunts peaks later in the light curve than native photorespiration and glycerate shunt. The carbon-fixing shunt is just about Rubisco-limited at 'saturating light' (I =1500$\mu E\ m^{-2}\ s^{-1}$). The reason is not that the synthetic shunts use light more efficiently (which they do), but that their limitation by Rubisco/CO_2 only kicks in at a higher level (because $A_{rbc}^{fix} > A_{rbc}^{nat} > A_{rbc}^{nat}$, where the superscript indicate the carbon-fixing shunt, carbon-neutral shunts and native photorespiration respectively). The higher A_{rbc}, the less it is limiting, and the curve is dominated by ATP-limitation. Thus our first conclusion is that our synthetic pathways should lead to higher net fixation rates (for the present time ignoring limitation by enzymatic activities other than Rubisco). This result does not depend on Rubisco kinetic parameters but is largely a consequence of the non-negativity of α. The second conclusion is that the advantage of the synthetic pathways should be greater the lower C_i falls.

[1] Since we are only concerned with situations where a photorespiration pathway operates alongside the Calvin cycle, and never without it, we will hereafter no longer explicitly write 'paired with the Calvin cycle' whenever we mention 'the activity' or 'the fixation rate' of a photorespiration pathway.

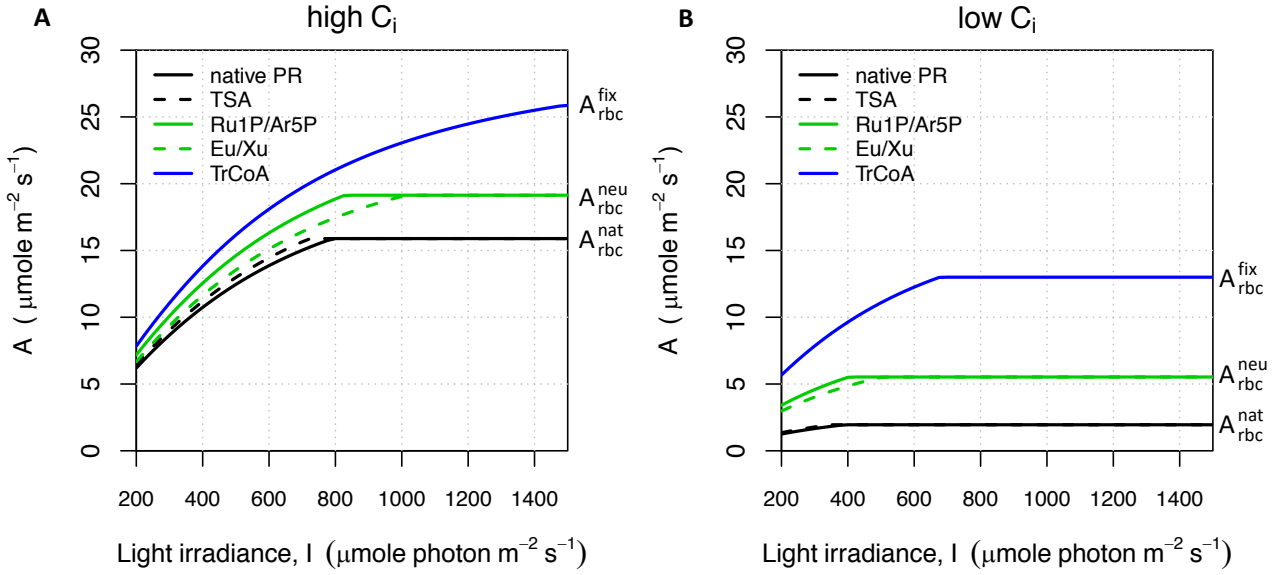

Figure 5: Light response curves of the restricted kinetic-stoichiometric model. A: Light response curves at high intercellular CO_2 concentration (C_i =8 μM). B: Light response curves at low intercellular CO_2 concentration (C_i =2 μM). Net carbon fixation rates of photosynthesis, i.e. the Calvin cycle paired with a photorespiration pathway, are plotted against light irradiance. In the restricted kinetic-stoichiometric model, the net fixation rate A^* is the minimum of the Rubisco-limited and the light-limited rate (here: ATP limited). The five pathways (native photorespiration, glycerate shunt, Ru1P/Ar5P shunt, Eu/Xu shunt, carbon-fixing shunt) are coloured according to the legend. The parameters for these plots can be found in Table 3. The values of the Rubisco-limited rate of the carbon-fixing shunt (A^{fix}_{rbc}), carbon-neutral shunts (A^{neu}_{rbc}) and native photorespiration (A^{nat}_{rbc}) are indicated.

3.2.4 Limitation by enzyme activities other than Rubisco

The FvCB steady-state model assumes that light and Rubisco/CO_2 are the only factors that limit the net carbon assimilation rate. In our mathematical framework, we can in addition treat three more limitations (see Section 3.1.3).

3.2.5 Limitation by a Calvin cycle enzyme

It is known that Calvin cycle enzymes other than Rubisco can limit photosynthesis. The best known example is sedoheptulose bisphosphatase (SBPase) [5]. From our theoretical analysis we know that this limitation would be more severe for native photorespiration than for the synthetic shunts. In native photorespiration, SBPase activity must carry one third of the flux generated by v_{carb} and one third of the flux generated by v_{ox}. This is the same as in the carbon-fixing shunt. However, the consumer model tells us that native photorespiration fixes only 2.5 carbons in the same time that the carbon-fixing shunt fixes 4 (i.e. the carbon-fixing shunt is 60% more carbon efficient at high C_i and saturating light). Therefore, with a fixed amount of Calvin cycle enzyme activity, a higher carbon fixation rate is achieved with the carbon-fixing shunt.

In contrast, the Ru1P/ Ar5P carbon-neutral shunts have a different mechanism of reducing the load of a

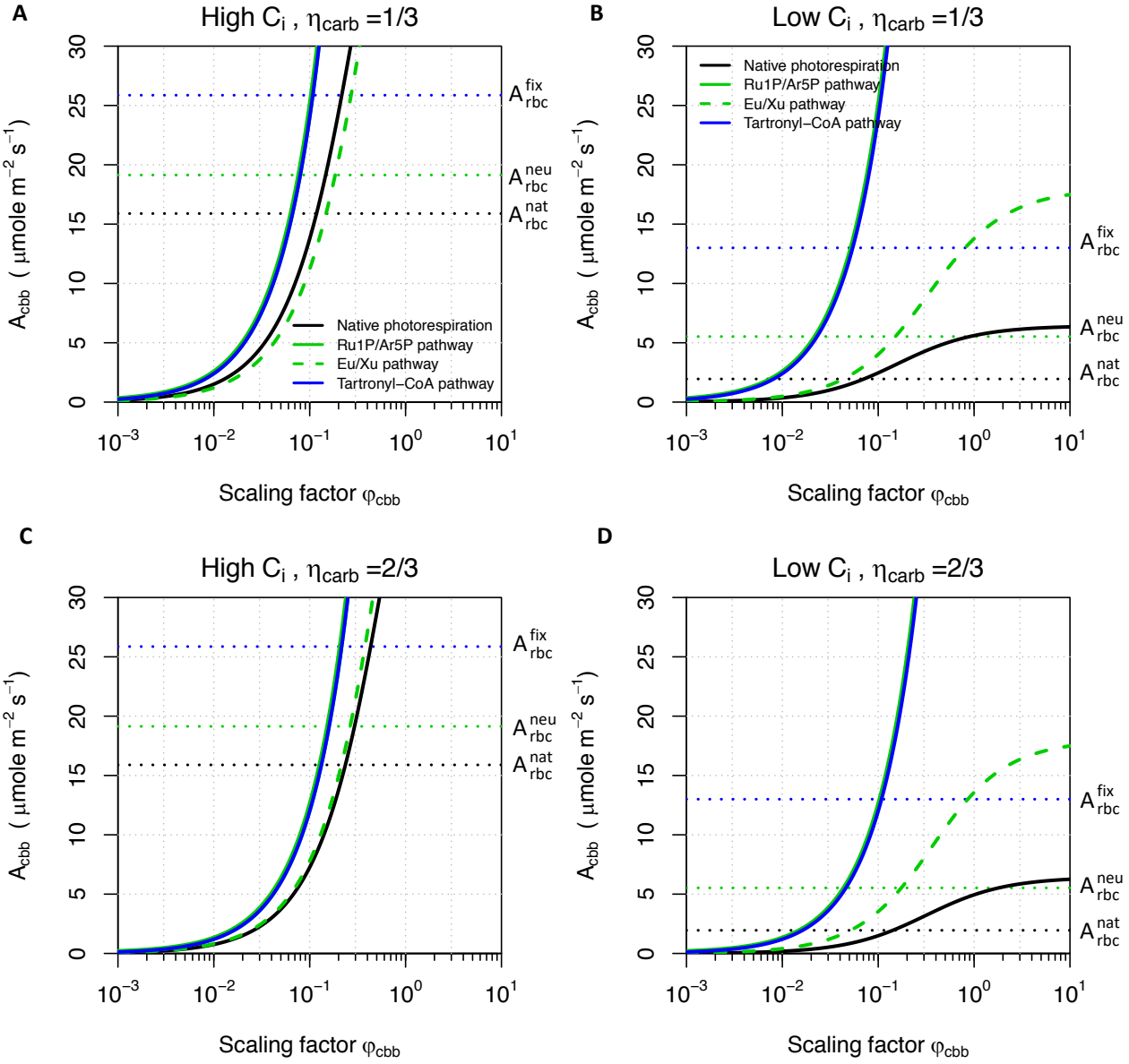

Figure 6: Limitation by a Calvin cycle enzyme. A and C: Carbon fixation rates assuming only a Calvin cycle enzyme activity is limiting (A_{cbb}), at high intercellular CO_2 concentrations (C_i =8 μM). B and D: A_{cbb} at low intercellular CO_2 concentrations (C_i =2 μM). The scaling factor φ_{cbb} expresses the activity of the Calvin cycle enzyme as the fraction of the maximal activity of RuBP carboxylase ($v_{cbb} = \varphi_{cbb} \cdot v_{carb\_max}$). The curve shown in panels A and B belongs to an enzyme that carries one third of the Calvin cycle flux ($\eta_{carb} = 1/3$), such as SBPase and FBPase. The curve shown in panels C and D belongs to an enzyme that carries two thirds of the Calvin cycle flux ($\eta_{carb} = 2/3$), such as aldolase and transketolase. Horizontal dotted lines represent the Rubisco-limited rate of the carbon-fixing shunt (A^{fix}_{rbc}, blue), carbon-neutral shunts (A^{neu}_{rbc}, green) and native photorespiration (A^{nat}_{rbc}, black, identical to glycerate shunt). The blue and solid green line are identical and are shifted slightly to the right to make them both visible.

potentially limiting Calvin cycle enzymes such as SBPase: the flux originating from photorespiration is completely redirected past all Calvin cycle enzymes that lie sequentially behind GAP (Fig. 2). Careful

analysis (Section 3.1.3) shows that the SBPase-limited rate would be same in the carbon-fixing and these carbon-neutral shunts and that this Calvin cycle-limited rate (A_{cbb}) is independent of the C_i. This analysis applies equally to FBPase, aldolase and transketolase (for all of these $\eta_{carb} = \eta_{ox}$ in native photorespiration and the carbon-fixing shunt and $\eta_{ox} = 0$ in the Ru1P/Ar5P carbon-neutral shunts, see Table 2).

To illustrate the effect of a limiting Calvin cycle enzyme, we define the scaling factor φ_{cbb} (Section 3.1.3) that expresses the activity of a Calvin cycle enzyme in units of v_{carb_max}, the maximal carboxylation rate of Rubisco [2]. In Fig. 6, we plot the fixation rate A_{cbb} against φ_{cbb} for an enzyme like SBPase ($\eta_{carb} = 1/3$) and aldolase ($\eta_{carb} = 1/3$ - aldolase catalyses two reactions). We compare this to the pathway-dependent Rubisco-limited rate A_{rbc} (horizontal dotted lines). At the intersection of the A_{cbb} with A_{rbc} of the same pathway (e.g. the black solid line with the black dotted line), Rubisco becomes limiting, and at values of φ_{cbb} lower than this point, the Calvin cycle enzyme is limiting. We call the value of φ_{cbb} at the intersection point the threshold φ_{cbb}^{TH}. About 1/10 of the maximal activity of Rubisco is required for a Calvin cycle enzyme to be non-limiting in native photorespiration. At high C_i, also the carbon-fixing and carbon-neutral pathways require about 1/10 of v_{carb_max} to be at least as high as their respective A_{rbc}. In contrast, both synthetic pathways only require a much smaller fraction of v_{carb_max} at low C_i.

Although $\varphi_{cbb} \approx 1/10$ seems to be sufficient in all cases to support a pathway's Rubisco-limited rate, it is important to stress that the synthetic pathways are capable of supporting a higher absolute rate of carbon fixation than native photorespiration with the same φ_{cbb}. With a given amount of enzyme, the synthetic pathways achieve much higher rates of carbon fixation, especially at low C_i. In other words, our synthetic pathways are more parsimonious.

Activity	Full name	EC	Latzko	Peterkofsky	Normalised range
Rubisco	rubisco (CO_2)	4.1.1.39	0.9	150	1
PGAK	phosphoglycerate kinase	2.7.2.3	130	4500	30-140
GAPDH	GAP dehydrogenase	1.2.1.13	15	260	2-17
TPI	triose phosphate isomerase	5.3.1.1	110	1100	7-120
ALD	aldolase (F6P)	4.1.2.13	5.3	300	2-6
FBPase	fructose bisphosphatase	3.1.3.11	2.4	39	0.3-3
SBPase	sedoheptulose bisphosphatase	3.1.3.37	0.2	8	0.05-0.2
TK	transketolase	2.2.1.1	10	300	2-11
ISO	phosphopentose isomerase	5.3.1.6	16	510	3-18
EPI	phosphopentose epimerase	5.1.3.1	8.4	1600	9-11
R5PK	phosphoribulokinase	2.7.1.19	16	600	4-18

Table 4: Calvin cycle enzyme total activities. The datasets of Latzko [7] and Peterkofsky [8] were rounded to two significant digits. The activity of GAPDH is the geometric mean of two values in the original tables that were obtained with different co-factors. The normalised ranges (last column) were obtained by scaling each set separately with the activity of Rubisco. SBP aldolase activity was not measured. The units of Latzko and Peterkofsky are $\mu mole\,(\text{mg protein})^{-1}\,h^{-1}$ and $\mu mole\,(\text{mg chlorophyll})^{-1}\,h^{-1}$ respectively, while the combined activity is unitless.

[2] φ_{cbb} absorbs the v_{max} of an enzyme and all factors concerning the saturation with substrates and products and the thermodynamics driving force of the reaction [6]. Thus, a value of $\varphi_{cbb} = 0.1$ does not describe a single state, it could equally mean that the enzyme is saturated with substrate and the v_{max} is 1/10 of v_{carb_max}, or that the enzyme is only 10% saturated and the v_{max} is equal to v_{carb_max}. Maximal rates such v_{carb_max} are defined as $v_{max} = k_{cat}\,E_{tot}$, where E_{tot} is the total concentration (abundance) of enzyme.

In order to compare our theoretical results with measured activities of Calvin cycle enzymes in relation to Rubisco, we present two datasets from spinach in Table 4. Clearly the lowest v_{max} is the activity of SBPase (between 0.05 and 0.2 $\cdot v_{carb\_max}$). Overall the results in Table 4 indicate that SBPase activity in spinach that is most likely to be limiting (in agreement with e.g. [5]). The average activity calculated from the two datasets is very close to $\varphi_{cbb} = 0.1$, the threshold value of native photorespiration that we calculated from our model. The activity of SBPase will in practice be lower than the total activity shown in Table 4 because the latter are measured at full saturation at maximal substrate saturation and thermodynamic driving force. Thus, there is very good agreement between the model and experimental evidence. In contrast, both of our synthetic shunts achieve higher rates of carbon fixation because their A_{cbb} curve is shifted to lower values of φ_{cbb}, in other words they can do more with less. In summary, native photorespiration (and the glycerate shunt) are considerably more vulnerable to the limiting activity of a Calvin cycle enzyme such as SBPase.

3.2.6 Limitation by a photorespiratory enzyme

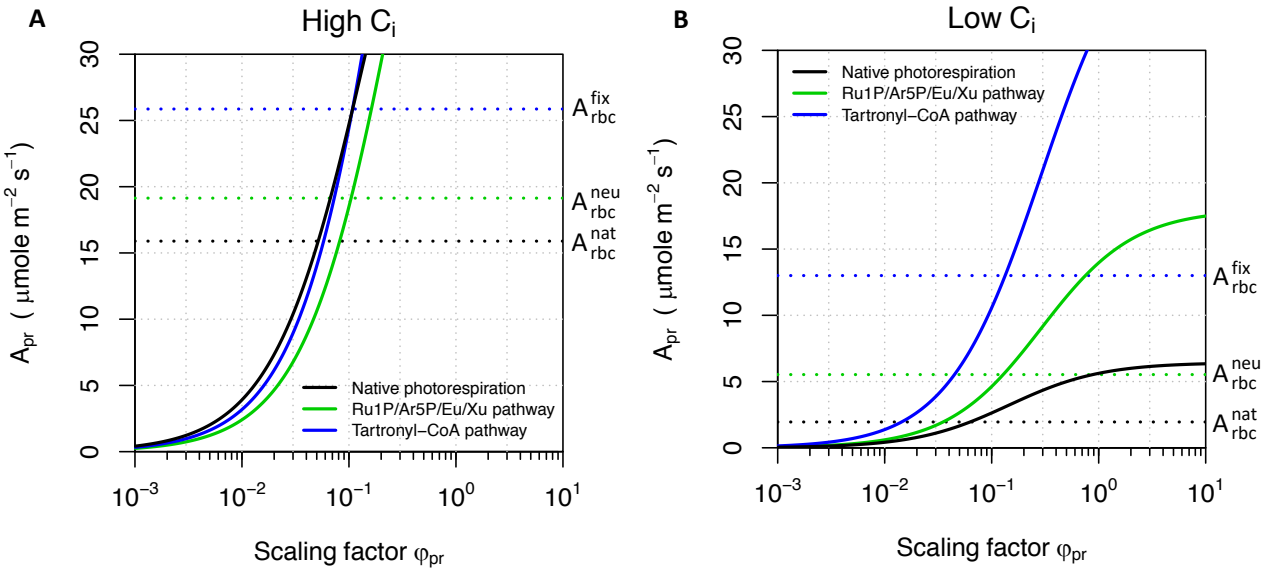

Figure 7: Limitation by a photorespiration enzyme. A: photorespiration (shunt) enzyme-limited carbon assimilation rates (A_{pr}) at high intercellular CO_2 concentrations (C_i =8 μM). B: photorespiration (shunt) enzyme-limited carbon assimilation rates at low intercellular CO_2 concentrations (C_i =2 μM). The scaling factor φ_{cbb} expresses the activity of the shunt enzyme as the fraction of the maximal activity of RuBP carboxylase ($v_{cbb} = \varphi_{cbb} \cdot v_{carb\_max}$). The native photorespiration curve shown belongs to an enzyme that carries one half of photorespiration flux ($\epsilon = 1/2$), whereas in the two synthetic pathways the enzyme is assumed to carry all of v_{ox}. The glycerate shunt is identical to native photorespiration. Horizontal dotted lines represent the Rubisco-limited rate of the carbon-fixing shunt (A^{fix}_{rbc}, blue), carbon-neutral shunts (A^{neu}_{rbc}, green) and native photorespiration (A^{nat}_{rbc}, black, identical to glycerate shunt).

The enzymes of an synthetic pathway need to be expressed at a sufficient level to achieve the improvements calculated in Section 3.2.3. Equally, in native photorespiration, also the non-Calvin cycle enzymes need to be expressed in sufficient amounts to achieve a Rubisco or light-limited fixation rate. In the following we will calculate this level of activity relative to Rubisco's v_{carb_max}.

The application of this principle to the synthetic pathways is straight-forward since they consist of two linear branches that carry equal flux (since RuBP oxygenase creates equal amounts of PGA and G2P, 2-phosphoglycolate) and are eventually combined in a 1:1 condensation reaction. Thus all enzymatic steps carry the same flux, v_{ox}. In contrast, the description of native photorespiration is not as straight-forward because the flux decreases from v_{ox} to $0.5\,v_{ox}$ in the middle of the G2P branch at the point of glycine condensation. We solve this problem by taking a conservative approach and assuming that in native photorespiration and the glycerate shunt, the limiting enzyme needs to only support $0.5\,v_{ox}$.

Theoretical consideration show that, at low C_i, the fixation rate A_{pr} of synthetic pathways is always higher than native photorespiration (and glycerate shunt). This is illustrated in Fig. 7B. However, at high C_i (Fig. 7A) and low values of φ_{pr} native photorespiration performs almost identically to the carbon-fixing shunt and slightly better than the carbon-neutral shunts. We again compare the value of φ_{pr}^{TH} at which the photorespiration-limited rate equals the Rubisco-limited activity: At high C_i this value for all pathways is between 1/10 and 1/20. At low C_i, the main difference is that the two synthetic pathways reach the level of A_{rbc} of native photorespiration much earlier, at $\varphi_{pr}^{TH} = 1/28$ and $\varphi_{pr}^{TH} = 1/69$ for carbon-neutral and carbon-fixing pathways. In summary, the synthetic pathways are less likely to be limited by a PR enzyme at low C_i which is the more relevant condition. At high C_i all pathways are relatively similar in performance.

3.2.7 Limitation by a photorespiration carboxylase

The carbon-fixing pathway contains an enzyme that is a carboxylase. Unlike all other enzymes except Rubisco, this enzyme depends directly on chloroplast CO_2 concentration. For this reason, we separate the saturation with CO_2 from the saturation with all other metabolites (Eq. 54) which is described by φ_{cbx}. The effective Michaelis constant for CO_2 is expected to lie close to $10\,\mu M$ (see Section 3.1.4, equivalent to a K_M of 1mM for bicarbonate). However, the flux in photorespiration shunt depends on RuBP oxygenase. Therefore, the situation may become critical at low values of x where v_{ox} is moderately increased (disinhibited), but the rate of the carboxylase is severely reduced.

This is indeed what we see in Figure 8B: at low C_i the scaling factor φ_{cbx} needs to be 2.6 (i.e. the rate needs to be 2.6 times Rubisco's maximal carboxylation rate) to reach the Rubisco-limited rate of the carbon-fixing shunt. However, it is not necessary to reach to theoretical maximum of A to achieve an improvement. To reach the carbon-neutral's theoretical maximum only one third of v_{carb_max} is required, and to compete with A_{rbc} of native photorespiration, only one tenth. The values are considerably higher than for a non-carboxylase shunt enzyme (Fig 7B), where the three values were 1/9, 1/17 and 1/19. Thus, to achieve the same level of net carbon fixation as the carbon-neutral pathway, the carboxylase of the carbon-fixing pathway needs to have six times more activity than any non-carboxylase enzyme.

At high C_i (Figure 8A), the requirements for the rate of the carboxylase are also considerable: 1/3 of v_{carb_max} to match its own A_{rbc}, 1/5 of v_{carb_max} to match the A_{rbc} of the carbon-fixing pathway and 1/7 of v_{max} to match the A_{rbc} of native photorespiration. These values are much closer to the requirements of a non-carboxylase enzyme in either of the synthetic shunts. What is required to reap the full benefits of the carbon-fixing shunt is about 3 times the activity of SBPase.

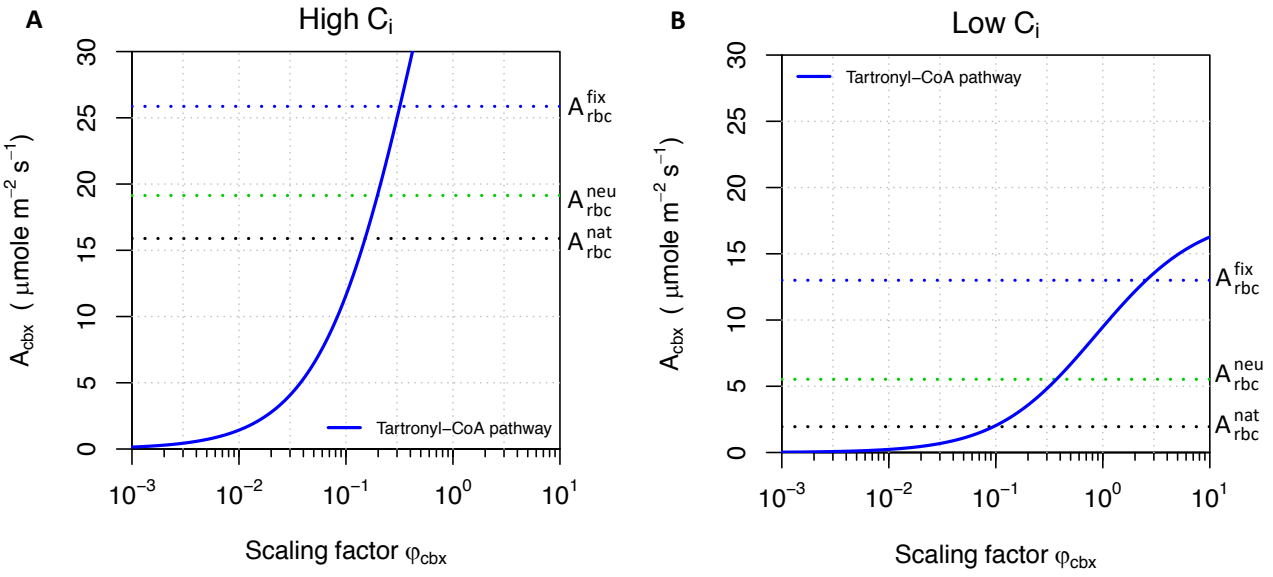

Figure 8: Limitation by a photorespiration carboxylase. A: photorespiration-carboxylase-limited carbon assimilation rates (A_{cbx}) at high intercellular CO_2 concentrations (C_i =8 μM). B: photorespiration-carboxylase-limited carbon assimilation rates at low intercellular CO_2 concentrations (C_i =2 μM). This enzyme only exists in the carbon-fixing pathway. It is assumed to have an apparent Michaelis constant for CO_2 of 10 μM (which corresponds to a K_M of 1 mM for HCO_3^-, see Section 3.1.3). The scaling factor φ_{cbx} expresses the activity of the carboxylase as the fraction of the maximal activity of RuBP carboxylase ($v_{cbx} = \varphi_{cbx} \cdot v_{carb\_max}$). Horizontal dotted lines represent the Rubisco-limited rate of the carbon-fixing shunt (A_{rbc}^{fix}, blue), carbon-neutral shunts (A_{rbc}^{neu}, green) and native photorespiration (A_{rbc}^{nat}, black, identical to glycerate shunt).

4 Conclusions

We have developed a mathematical model of plant photosynthesis that confirms the advantages of carbon-neutral and carbon-fixing photorespiration shunts over native photorespiration and previously suggested shunts. We clearly show that both carbon-neutral and carbon-positive shunts are significantly better in terms of net carbon fixation rate than native photorespiration, under all conditions that were examined. These conditions include high and low light and plants reacting to water shortage by closing their stomata.

In addition to light and water limitation of the net carbon fixation rate we investigated limitation by Calvin cycle enzymes, e.g. SPBase, and limitation by photorespiration enzymes proper. Our analysis shows that there are additional benefits of synthetic shunts that could give rise to a substantial increase in the carbon fixation rate.

Thus, our model very strongly supports the notion that replacing native photorespiration with carbon-neutral or carbon-positive shunts should be beneficial to C3 plants, especially in more challenging environmental conditions.

Our model is theoretically well founded and applicable to any conceivable photorespiration shunt.

References

[1] G. D. Farquhar, S. von Caemmerer, and J. A. Berry. A biochemical model of photosynthetic CO2 assimilation in leaves of C 3 species. *Planta*, 149(1):78–90, Jun 1980.

[2] R. Kebeish, M. Niessen, K. Thiruveedhi, R. Bari, H. J. Hirsch, R. Rosenkranz, N. Stabler, B. Schonfeld, F. Kreuzaler, and C. Peterhansel. Chloroplastic photorespiratory bypass increases photosynthesis and biomass production in Arabidopsis thaliana. *Nat. Biotechnol.*, 25(5):593–599, May 2007.

[3] S. von Caemmerer. Steady-state models of photosynthesis. *Plant Cell Environ.*, 36(9):1617–1630, Sep 2013.

[4] G. D. Farquhar and S. Wong. An empirical model of stomatal conductance. *Functional Plant Biology*, 11(3):191–210, 1984.

[5] S. Lefebvre, T. Lawson, M. Fryer, O. V. Zakhleniuk, J. C. Lloyd, and C. A. Raines. Increased sedoheptulose-1,7-bisphosphatase activity in transgenic tobacco plants stimulates photosynthesis and growth from an early stage in development. *Plant Physiology*, 138(1):451–460, 2005.

[6] E. Noor, A. Flamholz, W. Liebermeister, A. Bar-Even, and R. Milo. A note on the kinetics of enzyme action: a decomposition that highlights thermodynamic effects. *FEBS Lett.*, 587(17):2772–2777, Sep 2013.

[7] E. Latzko and M. Gibbs. Measurement of the intermediates of the photosynthetic carbon reduction cycle, using enzymatic methods. *Meth. Enzymol.*, 24:261–268, 1972.

[8] A. Peterkofsky and E. Racker. The reductive pentose phosphate cycle. III. Enzyme activities in cell-free extracts of photosynthetic organisms. *Plant Physiol.*, 36(4):409–414, Jul 1961.

[9] A. Bar-Even, E. Noor, N. E. Lewis, and R. Milo. Design and analysis of synthetic carbon fixation pathways. *Proceedings of the National Academy of Sciences*, 107(19):8889–8894, 2010.

[10] F. L. Smith and H. A. H. Avoid common pitfalls when using henry's law. *Chemical Engineering Progress*, pages 33–39, Sept 2007.

[11] D. T. Hanson, S. S. Stutz, and J. S. Boyer. Why small fluxes matter: the case and approaches for improving measurements of photosynthesis and (photo)respiration. *J. Exp. Bot.*, 67(10):3027–3039, May 2016.

[12] H. N. Po and N. M. Senozan. Henderson-Hasselbalch Equation: Its History and Limitations. *Journal of Chemical Education*, 78:1499, November 2001.

[13] R. Roy, L. Roy, K. Vogel, C. Porter-Moore, T. Pearson, C. Good, F. Millero, and D. Campbell. The dissociation constants of carbonic acid in seawater at salinities 5 to 45 and temperatures 0 to 45°c. *Marine Chemistry*, 44(2-4):249–267, 1993.

[14] F. J. Millero. Thermodynamics of the carbon dioxide system in the oceans. *Geochimica et Cosmochimica Acta*, 59(4):661 – 677, 1995.

[15] B. Alberts, A. Johnson, J. Lewis, M. Raff, K. Roberts, and P. Walter. *Molecular Biology of the Cell, 4th edition.* Garland Science, New York, 2002.

[16] R. A. Alberty, A. Cornish-Bowden, R. N. Goldberg, G. G. Hammes, K. Tipton, and H. V. Westerhoff. Recommendations for terminology and databases for biochemical thermodynamics. *Biophys. Chem.*, 155(2-3):89–103, May 2011.

[17] S. von Caemmerer. *Biochemical models of leaf photosynthesis*. Csiro publishing, 2000.

[18] X. Yin, M. Van Oijen, and A. H. C. M. Schapendonk. Extension of a biochemical model for the generalized stoichiometry of electron transport limited c3 photosynthesis. *Plant, Cell & Environment*, 27(10):1211–1222, 2004.

[19] S. von Caemmerer and W. P. Quick. *Rubisco: Physiology in Vivo*, pages 85–113. Springer Netherlands, Dordrecht, 2000.

[20] L. Taiz and E. Zeiger. *Photosynthesis: Physiological and ecological considerations*. 2002.

[21] Q. T. Ho, P. Verboven, X. Yin, P. C. Struik, and B. M. Nicolai. A microscale model for combined CO(2) diffusion and photosynthesis in leaves. *PLoS ONE*, 7(11):e48376, 2012.